Wireless Parking Detection System
Based on Sensor Fusion and IoT Communication

Yifan Zhuang

A thesis

submitted in partial fulfillment of the

requirements for the degree of

Master of Science in Civil Engineering

University of Washington

2019

Committee:

Yinhai Wang, Chair

Jeff Ban

Edward Donald McCormack

Program Authorized to Offer Degree:

Civil and Environmental Engineering

University of Washington

Abstract

Wireless Parking Detection System
Based on Sensor Fusion and IoT Communication

Yifan Zhuang

Chair of the Supervisory Committee:
Dr. Yinhai Wang
Civil and Environmental Engineering

With the constant growths of the automotive industry, traffic problems especially the parking problem is increasingly prominent. Currently, many parking facilities do not have enough capacity to support travelers' parking demand in urban areas. While building additional parking facilities is difficult for most cities, making optimized use of existing parking resources is a more practical solution. To this end, this study develops a wireless parking detection system for smart parking detection and management. The key hardware component of the system is a new wireless parking space detector named Smart Road Sticker (SRS), which is based on sensor fusion and Internet-of-Things communication technologies. New parking detection algorithms are developed and integrated into the SRS. Two field tests are conducted in representative scenarios. The experimental results and analyses demonstrate the effectiveness of this system

with high detection accuracy and low power consumption. Specifically, it achieves over 95% detection rate and over one-year battery life under various conditions.

TABLE OF CONTENTS

LIST OF FIGURES

LIST OF TABLES

ACKNOWLEDGEMENTS

I would first like to thank my master's degree study advisor Prof. Yinhai Wang. In this research, Prof. Wang provided a lot of guidance to help me figure out the key points of this research. When facing problems, no matter whether they are theoretical or practical, he was always glad to give me suggestions or cooperated with me to find solutions His rich theoretical knowledge and experience in practice significantly supported this research work.

And I appreciate the support and guidance from my committee members – Prof. Jeff Ban and Prof. Edward Donald McCormack. Their work further improved this research.

Then I would like to appreciate the support from Sound Transit in the project "A Multi-Sensor Solution for Sound Transit Parking Space Detection". They provided a perfect testing scenario for our parking detectors in the practical environment. In this project, the detector's performance is well evaluated.

Finally, I would also like to thank my colleagues at Smart Transportation Application and Research Lab at the University of Washington. They did not only give me advice on developing the detection system but also provided me a lot of support in the field tests. Without their work, it would be much harder to reach the research target.

Chapter 1. INTRODUCTION

1.1 PROBLEM STATEMENT

The traffic congestion has generated more and more negative impacts on people's daily life such as increasing travel time and costs. And it also increases the wastes of social resources and air pollution. Thus, traffic congestion becomes one of the most critical problems to be solved for most cities. Traffic congestion happens when traffic volume is higher than the capacity. Although the causes of traffic congestion are complex, they can be generally divided into short-term causes and long-term causes. Terrible weather and traffic incidents can lead to short-term congestion, while roadblock by work zones and insufficient transportation infrastructure can bring long-term congestion. The parking facilities including both parking garages and street parking are part of the transportation infrastructure. Therefore, the insufficient parking facility is considered as one of long-term causes of the traffic congestion. Currently, there are three challenges facing the research and engineering fields regarding parking.

1) Fast-growing Demands

Based on relevant surveys, more than 30% of travelers are looking for parking spaces during rush hours, which is an important issue influencing the traffic flow [1]. With the expansion of cities, the distance between residential areas and working locations is farther than before, which makes travelers rely more on driving than walking or cycling. Although public transportation has been well developed, travelers who do not live near the bus stops or need to transfer to get their destination are more likely to drive their private vehicles. The disequilibrium between the fast expansion of cities and inadequate public transportation lead to rising demand of driving private

vehicles. As a result, there is a fast-growing demand for parking spaces especially in urban areas accompanying the expansion of cities.

2) Limited Resources

The challenge of limited resources can be classified into two aspects – inadequate parking spaces [2] and out-of-date facilities. During the work time, the parking capacity in urban areas cannot meet the parking demands for all vehicles. However, during the rest of the time, most parking spaces are vacant. For street parking, the optimal occupancy rate is 85% [3]. Considering the land in the urban area is limited and parking covers the most surface area compared to other land uses in central business districts [4], it is challenging to expand parking space in urban areas. The second aspect is the out-of-state parking facilities which may not be suitable for new vehicles. At present, more electric vehicles are on the road and have the demand for charging stations. The parking facilities without charging stations are less attractive to these vehicles, which will lead to their concentration in some specific parking facilities.

3) Insufficient Parking Information

Currently, the parking space detection system is not widely applied in parking facilities in US cities. Even though there are surveillance cameras installed, their basic tasks are either monitoring facility safety or counting in/out vehicles. The parking occupancy distribution information is still missing. As a result, parking agents cannot provide guidance to drivers and inform them where available spaces are. Meanwhile, insufficient parking information will also increase the search time for drivers even if there are available spaces. All parking spaces can be seen as a list where the empty space is the searching target. Without occupancy information, this list is unsorted. And

the only search strategy is linear search which sequentially checks each position until finding the target or the whole list has been searched [5]. It has the lowest efficiency in most cases with the complexity of $O(n)$. The occupancy distribution information can make this array sorted. Before that, there is no better method for speeding up the search.

In order to improve the operation efficiency of the parking system and reduce the search time, there is an urgent demand from both parking agencies and drivers to have a smart parking system to provide the available parking space information [6].

1.2 PROPOSED SOLUTION

The smart parking system, which is a part of the Intelligent Transportation System (ITS), is an effective solution to the parking problem. The ITS is defined as a system integrating traveler, road and vehicle together to improve the efficiency and safety [7]. And the smart parking system focuses on optimizing the parking facilities by making them smarter to sense the parking status and to publish parking information to both agencies and drivers. The foundation of the smart parking system is its detection system. The standards for the detection system are concluded into three parts – high accuracy, long battery life and high reliability.

1) High Accuracy

Compared to detection systems for traffic flow detection such as inductive loop detectors and microwave radar, the detection system for parking application has a higher accuracy standard. For each parking space, there are only two detection results. When the parking facility is busy, even one detection error may generate negative impacts on the overall detection performance. Users are

less likely to speak highly of the performance of the detection system when the results are correct. But there is a great possibility for them to blame the system and give a low rank on the internet when the detection results are wrong. The negative comments accumulate more easily. In summary, the parking detection system needs to be very accurate.

2) Long Battery Life

In most parking facilities, there is no specific power interface for the detection system. In addition, the detection unit may be installed at a position which is good for detection accuracy but far from existing power interface. As a result, extending power wires will be necessary. However, extending power wires is a challenge since extra work is required. And it will thus increase cost of material and labor. If the sensor is supported by batteries instead of external power supply, the battery life becomes the most critical indicator to assess its durability. To a large extent, long battery life indicates a long maintenance period of replacing the battery component or the sensor unit.

3) High Reliability

Besides the detection accuracy and battery life, reliability is also an important evolution index. All detection systems suffer the reliability problem since they are exposed to various severe conditions. For example, the oil stain and sediment will erode the detection unit. The building can block the wireless communication between the detection unit and the base station. And the vehicle rolling may also damage the detection unit on the ground surface. In laboratory testing, the evaluation work mainly focuses on accuracy and functionality. In practical applications, the reliability is equally important to accuracy and battery life. What's more, high reliability also implies less maintenance after installation.

The state-of-the-art parking detection systems often rely on a single sensor so that the typical sensor's drawbacks also limit the application of the parking detection system. Therefore, the sensor fusion method is significant and becomes a popular solution to further improve the accuracy under various conditions. Recently, the Internet-of-Things (IoT) communication technology has been widely used and contributes to the deployment flexibility. Focusing on parking space detection, this study designs, builds and tests a wireless parking detection system based on sensor fusion and IoT communication technologies. The core of this parking detection system is named Smart Road Sticker (SRS). The major contributions of this research work have three perspectives. The first one is designing and making the Printed Circuit Board (PCB) specific for the parking space detection. And this PCB integrating multiple modules achieves three targets – high detection accuracy, low power consumption as well as long communication distance at the same time. The second one is improving the existing parking detection algorithm based on magnetic sensor and ultrasonic sensor to adapt to different application scenarios. The third one is proposing innovative parking detection algorithms based on light sensor and sensor fusion algorithm.

. This paper develops both hardware and software of SRS as well as conducting two field tests to evaluate the performance of SRS. Chapter 2 summaries previous research work on vehicle detection. And Chapter 3 introduces the hardware design including the hardware framework, function modules, and case design. Then Chapter 4 describes the software design, including detection algorithms based on three different sensors and two sensor fusion algorithms based on different sensor combinations. After developing both hardware and software, Chapter 5 firstly evaluates the power consumption of SRS. Then this chapter summarizes the results of two field tests conducted at two sites and problems exposed in each test. Finally, Chapter 6 concludes all research work done in this paper and makes a future plan for next-step development.

Chapter 2. LITERATURE REVIEW

The rapid development of the economy leads to the constant growth of vehicle in cities. And the huge number of vehicles make traffic congestion become one of the most severe problems in most big cities [8]. Not only does the traffic congestion waste much travelers' time [9], but also it increases air pollution [10] and speeds up the consumption of social resources [11]. Therefore, finding a solution to traffic congestion is a super important topic, and it involves multiple research fields from theory to engineering, such as operation research [12], urban planning [13], sensor development, etc. Before optimizing the traffic status, the first step is collecting traffic information such as traffic flow speed and density. Thus, the traffic collection methods play a key role since its accuracy and timeliness are directly related to the ultimate optimization results. Currently, the traffic information collection methods can be classified into two categories based on the sensor mobility – stationary method and mobile method.

2.1 STATIONARY METHOD

The stationary method is the most common and widely used method. This method is defined as applying detectors at fixed locations to collect traffic information. The typical detectors in this method include inductive loop detector [14], microwave detector [15], video camera [16], acoustic sensor [17], light sensor [18], magnetic sensor [19], etc. The advantage of the stationary method is its high accuracy in the detection range. But the disadvantage is also obvious that the detection range is relatively small since it cannot move.

The inductive loop detector was firstly used in the 1960s [20] and then widely applied in different scenarios such as identifying rear-end collision risks [21] and speed estimation [22]. The

operating principle is detecting the increase or decrease of loop inductance caused by passing vehicles [23]. However, the weakness lies in its installation and reliability. The installation and maintenance are complicated. And wire loops are also vulnerable when subject to stresses of both traffic and temperature [24].

Comparing with the inductive loop detector, the microwave radar reduces the complexity of installation and maintenance because it is mounted on the roadside pole or hang over the road. In order to detect the vehicles on the roads, microwave radar firstly sends energy in the direction to the roadway and then analyzes the wave reflected from the object on the roadway [15]. One important application of the microwave radar was vehicle detection and classification. Jianxin Fang, etc. applied K-band unmodulated continued-wave radar to achieve multiple detection tasks simultaneously including the speed measurement and vehicle classification [25]. However, the microwave detector suffers the problem that it is easily influenced by nearby metal infrastructure and occlusion of targets.

Similar to the microwave radar, the ultrasonic sensor also sends energy toward the target and then calculates the interval between the sending and receiving time. But the difference lies in that the ultrasonic sensor uses the sound wave instead of the radio wave whose frequency is much higher. S. H. Jeong, etc. designed a parallel parking system using the ultrasonic sensor [26]. The ultrasonic sensor was installed on the roadside to detect the distance between the vehicle and the road shoulder. Amin Kianpisheh, etc. used the ultrasonic sensor for indoor parking space detection [27]. The ultrasonic sensor was installed on top of each space to measure the distance between the ground and floor. If a vehicle occupied this parking space, the distance would decrease. However, different shapes of vehicles may influence the detection results since they have different ultrasonic wave reflections. In order to further improve the detection accuracy of the ultrasonic sensor, Wan-

Joo Park, etc used the multiple-echo function [28]. Based on experiment results, the multiple echo function's variance was 55% less than the single echo function when the radial resolution was 70cm. The disadvantage lies in that the probe of the ultrasonic sensor is easily affected by ice or other sundries.

The surveillance video camera is now one of the most popular detectors in the traffic system which can collect more abundant traffic information than other methods [29]. Different algorithms have been studied such as Support Vector Machine (SVM) classifier [30] and Convolutional Neural Network (CNN) [31]. Based on the inter-space correlation of parking space, Qi Wu, etc. combined the SVM classifier and Markov random field to detect the empty space [32]. Moreover, Orhan Bulan, etc. further developed the SVM to detect on-street parking occupancy and achieved real-time performance at five frames per second [33]. However, the main challenge faced by the video system is the low detection accuracy in some poor light conditions like rainy and foggy days.

The acoustic sensor captures the acoustic feature of vehicles when they approach or move away. Shigemi Ishida, etc. build a vehicle count system containing two microphones [34]. The detection algorithm was using dynamic-time-wrapping sound map. Jiagen Ding, etc. took deep research on the acoustic sensor for vehicle detection [35]. In their research work, the first step was characterizing the acoustic signal by Fast Fourier Transform. Then two algorithms were proposed in the frequency domain – the Adaptive Threshold Algorithm and the Min-max Algorithm. In order to collect more traffic information such as localization of traffic congestion, the acoustic sensor network was also deployed along the roadside [36]. The main reason that the acoustic sensor is not widely used is that the vehicle acoustic signal is easily submerged by the background noise from other sources.

When the detector is occupied by a vehicle, the light received by the detector will be blocked. The illuminance will thus drop dramatically compared to the unoccupied condition. As a result, the light sensor was also used for vehicle detection [37, 38]. Two kinds of light are commonly used for detection – visible light and infrared light. Mamta Bachani, etc. made use of both kinds of lights for vehicle detection [39]. In their research, the visible light sensor was a passive sensor to receive the visible light. And the infrared light sensor was a proactive sensor including two parts. The first part was a transmitter to send infrared light and the second part was a receiver for the reflected infrared light. But the light sensor suffers several crucial shortcomings. Firstly, the light change scale is uncertain under different light conditions. Secondly, the fluctuation of the environmental light may generate great noise and submerge the main signals especially when the environmental illuminance is low.

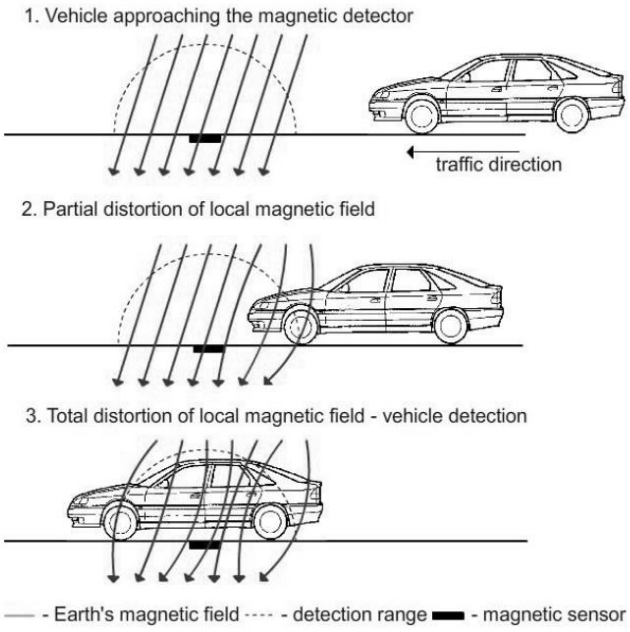

Figure 2.1 Magnetic Field Distortion Caused by a Vehicle [40]

The magnetic sensor is one of the most popular sensors for vehicle detection because of its high sensitivity and flexible deployment. The detection principle is measuring the magnetic field distortion caused by the vehicles in both horizontal and vertical dimensions [40]. And the distortion schematic diagram is shown in Figure 2.1. Based on Figure 2.1, the vehicle can greatly distort the magnetic field near the sensor. Cheung, Sing You [14] used the magnetic sensor node for both traffic measurement and vehicle classification. They analyzed different magnetic field patterns to classify different vehicle types. As a result, the vehicle detection accuracy was 99% and the vehicle length estimation was also greater than 90%. Based on the previous research work, Qing Wang, etc. built an adapted threshold state machine algorithm to overcome the shortage of magnetic field fluctuation [41]. And experiments were done on the roadside to detect vehicle on both adjacent and nonadjacent lanes. In order to improve the detection accuracy in the nonadjacent lane scenario, they applied the linear classification method. As a result, the detection accuracy of vehicles on adjacent lanes was more than 90%, while the accuracy on nonadjacent lanes was 40%. Vytautas Markevicius, etc. studied how the sensor positions influence the detection results and then compared 12 methods which were all based on signal peaks and their concurrence in time [42]. The 12 methods are shown in Table 2.1. Two best methods they found were method 2 and 10 which has the minimum error based on their experiments.

Beyond detecting vehicles on road, the magnetic sensor was also used to detect the parking space. Xiangke Guan, etc. studied the sensor application in different parking scenarios including both vertical and parallel parking [43]. The Relative Extremum Algorithm was applied, which used a state machine to detect the waveform features in the parking process. Jiagen Ding, etc. used an Adaptive Threshold Algorithm which made use of the time-domain energy distribution [44]. However, the magnetic field near the sensor is easily affected by other ferromagnetic materials

more than the vehicle over the sensor. The reinforced concrete and other vehicles passing by may generate disturbance on the magnetic signals.

Table 2.1 List of Detection Methods of Magnetic Sensor [42]

No.	Method
1	Z component peak detection
2	Z component cross-correlation
3	Module peak detection
4	Module cross-correlation
5	Vectorial deviation peaks
6	Vectorial deviation cross-correlation
7	Combined vectorial deviation peaks
8	Combined vectorial deviation cross-correlation
9	Kz criterion peaks
10	Kz criterion cross-correlation
11	Z peaks ± 50 readings of cross-correlation
12	Module peaks ± 50 readings of cross-correlation

In order to further improve the detection system and to make up for the disadvantages of every single sensor, the idea of sensor fusion was proposed by fusing multiple sensors. Some research work has been done in this field. Tatiana Bokareva, etc. combined the acoustic and magnetic sensor together [45]. Chellappa, Rama, etc. combined the acoustic and video sensor together [46]. Firstly, they used the acoustic sensor to get a rough estimate of target direction-of-arrival. Then the target's location would be refined by the video sensor. Fernando Garcia, etc. used the radar and video sensor for vehicle detection especially for detecting overtaking vehicles [47]. What's more, the studies about the fusion of laser scanner and video sensor were also done to improve the overall detection accuracy [48, 49].

For the sensor node mounted on the road surface, E. Sifuentes, etc. put forward a sensor fusion method combining the magnetic and light sensor. They wanted to extend the battery life by using the light sensor to trigger the magnetic sensor since the light sensor was more power efficient [50]. As a result, the results were impressive. If one node detected 4,320 vehicles a day, the battery life was about 1.5 years. If one node only detected 10 vehicles a day, the battery life could reach up to 30 years. Sai Ma, etc. did the research work on combining the magnetic and infrared distance sensor [51]. The infrared distance sensor worked as the secondary sensor trigger by the magnetic sensor and would determine the occupancy status. Most work focused on architecture design and validation tests rather than practical application. There is still a lot of work to be done including increasing the system robust in abnormal situations and improve power efficiency in some extreme environments to extend the battery life.

2.2 MOBILE METHOD

Different from the stationary method, the detector in the mobile method will change its position during the detection process. There are three popular mobile collection methods – the floating vehicles [52], onboard video sensors [53], and unmanned aerial vehicle (UAV) [54]. The floating vehicle data (FVD) is based on collecting vehicle position, speed, travel direction and time information from mobile phones or other in-vehicle GPS devices. Sven Maerivoet and Steven Logghe compared the FVD with data from single inductive loop detector [55]. The FVD can capture the large variations in travel times on roads containing intersections. One important application of FVD is detecting the traffic state. Based on minimizing two FVD messages, the information on typical traffic incidents could be recognized [56]. However, the detection accuracy of the floating vehicle method remarkably depends on the penetration rate of floating vehicles and

the signal quality [57]. In other words, floating vehicles are just discrete points in the traffic flow. If there are not enough points, it is hard to use them to estimate the traffic flow parameters like traffic flow density. In many cases, the FVD was sparse in both time and space dimensions, some research work thus has been done on extracting path information from sparse data [58]. Since the FVD highly depends on the location information, it suffers the challenge of inaccuracy when either GSM or GPS signal is weak.

Different from the FVD which is just location information, the onboard video combines the location and video information. The freeway traffic surveillance can greatly benefit from the onboard video as a supplement to stationary methods like inductive loop detector and video camera by detecting traffic between two stationary detection positions [59]. Different frameworks were proposed to improve the detection accuracy [60, 61]. Another scenario for onboard video is traffic sign localization and recognition [62, 63], which makes contribution to the autonomous vehicle to sense the surrounding environment. For example, the onboard system could warn the driver for inappropriate actions or take actions autonomously based on the traffic sign [64]. However, similar to stationary video method, the onboard video method shares the same weakness that it is easily affected by different light conditions.

Recently, UAV-based traffic sensing method has been receiving attention in transportation research studies. It has a “bird’s eye view” and better maneuverability than the ground vehicle. These two features are beneficial to traffic surveillance [65]. Based on the advantages shown above, the UAV was used to detect vehicles and people under different scenarios [66]. The nature of UAV detection is still a video detection but had a different view. Therefore, the computer vision methods were widely used as well, such as optical flow [67] and CNN [68]. Compared to other video detection scenarios, the UAV’s scenario was simpler, and its detection performance was

better and more stable. However, besides challenges faced in other video methods, the UAV technology has several more concerns such as the short battery life and privacy issue [69].

More than three mobile methods listed above, some researchers studied other sensors on mobile platforms. Some work focused on installing the ultrasonic sensor on the side of a vehicle as a mobile detector [70, 71]. The original task was detecting the empty parking space on the roadside. When there was an empty space, the distance between the vehicle and the roadside would change. What's more, in the autonomous vehicle setting, the laser sensor on the vehicle was used to scan the surrounding environment [72]. Although all mobile methods have a larger detection range than corresponding stationary methods, they cannot monitor one position all the time and provide real-time transportation information of that position because there is a scan period, which depends on the detection range and speed.

The parking space detection is an important part of the smart parking system which can improve the operation efficiency of parking facilities and also help ease the traffic congestion. And the essence of parking space detection is the vehicle detection. A lot of research work has been done on developing the parking detection system in the perspectives of both hardware devices and detection algorithms. Based on previous research work, this paper proposes an innovative parking detection system, whose core component is SRS. Then the next two chapters will introduce the hardware and software designs of SRS respectively, which are the most important parts in this research.

Chapter 3. HARDWARE DESIGN

The SRS is the central part of the parking detection system, which integrates the sensor fusion and IoT communication technologies. In order to reduce the dimension of the SRS and improve the detection accuracy and power efficiency, a specific PCB and two cases for all weather protection are designed for the parking application.

The SRS utilizes advanced sensor-fusion technologies and IoT communication mechanism to achieve three targets of high detection accuracy, long battery life and long communication distance at the same time. This chapter is developed in three sections. Firstly, Section 3.1 summarizes the alternative designs of SRS and challenges faced by the parking detection system. Section 3.2 then describes the electronic design of different modules, including the operating principle, module function and electronic components selection. At last, Section 3.3 describes case design including the materials and dimensions.

3.1 ALTERNATIVE DESIGNS

Just as discussed in Chapter 2, the traffic detectors include magnetic sensor, radar sensor, video sensor, etc., which have been widely applied in different scenarios such as freeways and parking facilities. Different sensors have various strengths but also own some drawbacks which limit their usages. For example, the magnetic sensor is sensitive to the vehicle existence but easily influenced by surrounding ferromagnetic materials. In common, it works well in the open area but does not have a good performance in the building since there is various magnetic disturbance around such as reinforced concrete [73]. The ultrasonic sensor is always used in detecting distance change, but its probe is usually blocked in outdoor environment. In recent years, though the wide application

of video sensor for all kinds of purposes, there are still some inherent shortcomings. For example, it is easily influenced by the environmental light, which could not be compensated by correction algorithms on the software level.

Considering that the single sensor may be limited to one or multiple application scenarios, it is important and necessary to develop a vehicle detection system by fusing different sensors to further increase the detection accuracy. In this paper, the research scenario is chosen in the parking facility for parking space detection. Therefore, the basic tasks are detecting the occupancy of each slot and then sending occupancy status information to the nearby control center immediately when there is an occupancy status change. In order to detect each parking slot, the concept of SRS is proposed. The SRS idea comes from the solar road stud which is mounted on the road surface to delineate road edges and centerlines. Instead of illumination function, the SRS integrates multiple sensors and IoT communication, which empower the SRS with the function of detection and communication.

In contrast to previous parking detectors, the SRS has been deeply improved in the three perspectives – fundamental cost, detection performance and communication range. Firstly, the average cost of each unit is reduced contributed by the advanced sensing and communication technologies. And low cost will also benefit large-scale applications. Secondly, the sensor fusion method improves the average detection accuracy in the hardware perspective by providing more accurate and reliable data. Lastly, the proper IoT communication extents the transmission distance up to $500m$ when only using a zero-gain antenna in an open area. The details of three improving perspectives are described below.

1) Fundamental Cost

The total cost of SRS in its service life is divided into three sections – manufacturing, installation, and maintenance. The first section includes two parts – PCB and electronic components. The PCB only have two layouts with a dimension of $25 \times 63.5mm$. The cost is less than \$0.20 for each piece. Contributed by great progress in electronic technology, these components become much more cost-effective. And the sensor fusion also helps reduce the total cost. In the past, the high-accuracy sensor would take multiple-time costs in order to increase 5% accuracy for example. Benefit from sensor fusion technologies, the overall detection accuracy is not less than previous top accurate sensors with much lower cost. In addition, the super low-power consumption makes it possible to use a small-volume LiPo battery, such as $6{,}000\ mAh$ LiPo battery, to support the whole service life. The small-volume battery does not only reduce the cost of the battery itself, but also reduce the dimension of the case.

One notable feature of the SRS is its thin case with a height of only $30.5mm$. Therefore, it can be mounted on the ground surface using waterproof epoxy adhesive rather than drilling a hole. Based on previous practical experience, drilling holes takes a lot of time and labor. Drilling one hole usually takes more than 40 minutes on average, and also does some damages to the ground. The simple installation will reduce the whole cost.

2) Detection Performance

More than cutting down cost, the sensor fusion technology also promotes the detection accuracy in different scenarios. The existing vehicle detectors always use a single sensor. For example, the magnetic sensor is sensitive and energy-efficient. But it is easily interfered and hard for calibration. And the ultrasonic sensor can detect vehicle directly without computing intermediate variables. It

consumes too much power yet. In current applications, the ultrasonic sensor is always wired to the power source. In order to overcome challenges caused by single sensor's drawbacks, the SRS combines different sensors. One version of SRS applies the magnetic sensor and ultrasonic sensor to make up each other's weakness. The magnetic sensor is responsible for detecting the occupancy change and ultrasonic sensor as the secondary sensor then verifies the detection result and checks the parking status periodically. What's more, the detection algorithms based on the sensor fusion are developed to promote the integration of multiple sensors and to improve the detection accuracy under different conditions as well.

3) Communication Range

There are several IoT communication protocols with low power consumption which are possibly used for communication like Bluetooth Low Energy (BLE), ZigBee and Long Range (LoRa). The first two protocols have a higher transmission rate but much shorter communication distance. One great advantage of LoRa is that it can reach to very low receiver sensitivity (down to -134dBm), which is combined with an output power of +14dBm. In the ideal environment with a proper antenna, the communication distance can be 13 miles in Line-of-sight links and to 1 mile in Non-line-of-sight links. Although the transmission rate is as low as a few bytes per second, the packet size that the SRS will transmit is also small. And the SRS will send information packets when detecting parking status change and will report current status in a long cycle. Another advantage of LoRa is that its large capacity which can be up to 800 nodes when fully using all 8 channels. Also, the power consumption is $10.3mA$ in transmission mode and as low as $100nA$ in sleep mode. With the application of LoRa technology, the SRS can achieve the target of low-energy consumption and long-distance communication at the same time.

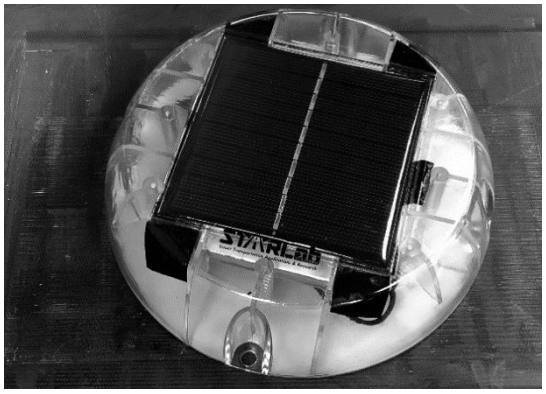

(a) SRS Version One

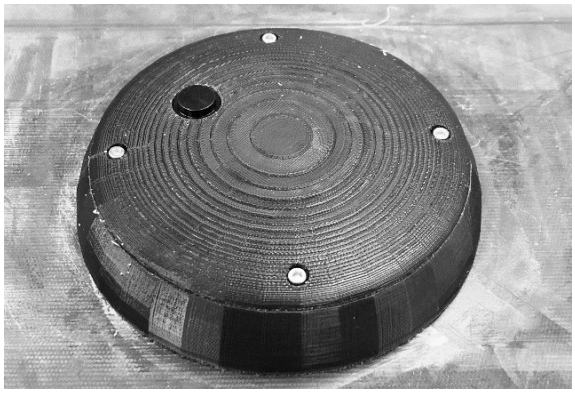

(b) SRS Version Two

Figure 3.1 Two Versions of SRS

Currently, two versions of SRS are designed and built, which are shown in Figure 3.1. The main difference between these two versions is the sensor combination while other components are totally the same. The first version (called SRS Version One) uses magnetic sensor and light sensor. This combination works well in an open area, but it is more easily influenced in the garage due to the reinforced concrete structure. The second one (called SRS Version Two) uses magnetic sensor and ultrasonic sensor. It has a better performance in the garage to detect the vehicles, but it is more easily influenced in the open area because of more sundries. Figure 3.1 (a) shows the SRS Version One. The magnetic sensor plays as the leading role in the detection process, while the light sensor assists the magnetic sensor to verify its detection result and makes up the missing detection by magnetic sensor. Figure 3.1 (b) shows the SRS Version Two which uses the magnetic sensor as the key sensor and the ultrasonic sensor to verify the magnetic sensor's detection result.

Based on Figure 3.1, it can be seen that the SRS Version One uses the transparent case in order to let the solar panel can receive the environmental light for power charging purpose. And the ultrasonic sensor probe is located at the upper left position and it is directly exposed to the air.

3.2 ELECTRONIC DESIGN

In the perspective of functionality, the SRS can be divided into four parts – sensor module, control module, power module and communication module. The structure diagrams of SRS are shown in Figure 3.2. Figure 3.2 (a) shows the structure diagram of SRS Version One while Figure 3.2 (b) shows the structure diagram of SRS Version Two.

The sensor module contains all sensors for vehicle detection purpose. The control module is responsible for controlling the sensor, processing raw data from sensors to compute the detection results. The power module supplies basic energy for this device. And the communication module transmits detection results to the nearby base stations. Different modules are connected by various protocols. The sensor module and CPU are connected via Inter-Integrated Circuit (I2C) bus and Analog-to-Digital Converter (ADC). The communication protocols depend on the sensor type. And the communication between CPU and communication module is using Serial Peripheral Interface (SPI). Considering there may exist a voltage fluctuation of power module when the environmental light is changing or battery voltage declines, the regulator is important to keep the power supply of the whole device stable.

According to Figure 3.2 (a) and (b), the only difference lies in the secondary sensor since the first sensor is magnetic sensor. For the secondary sensor, SRS Version One uses light sensor and SRS Version Two uses ultrasonic sensor. The other modules remain the same which simplifies the sensor change work by redesigning only the I/O ports and keeping the same power circuit. One important thing to be addressed is that this design requires that sensors should operate at the same voltage level. In this paper, all sensors operate at the $3.3V$. If the sensors have different operating voltages, additional power regulator and logic convertor will be required.

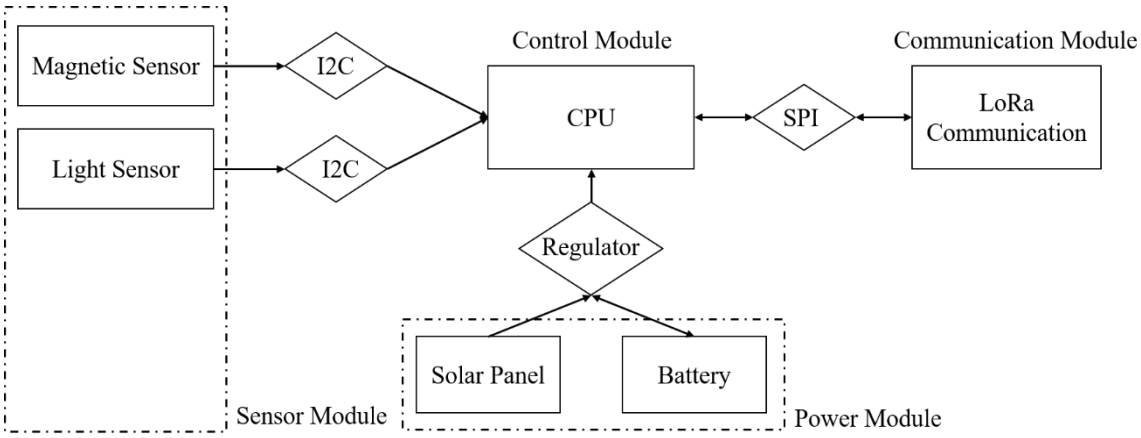

(a) Structure Diagram of SRS Version One

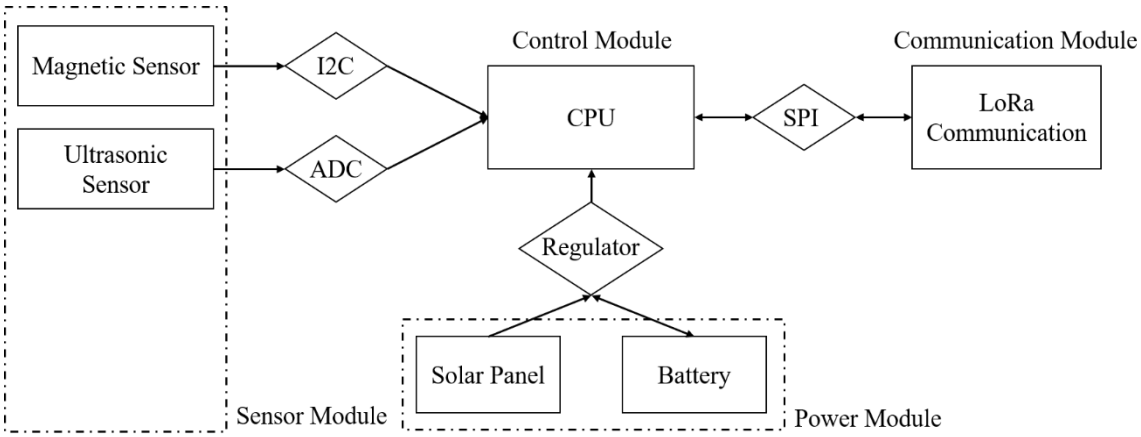

(b) Structure Diagram of SRS Version Two

Figure 3.2 Structure Diagram of SRS

The PCB of SRS is shown in Figure 3.3. Both Versions of SRS share the same basic PCB since only magnetic sensor is integrated on PCB. Based on functionality, the PCB can be mainly divided into four regions which are marked by boxes in Figure 3.3. They are sensor module (only magnetic sensor), power module, control module and communication module. In order to expand the PCB's compatibility to different secondary sensors, either the light sensor or ultrasonic sensor is not integrated into the board. These two secondary sensors are connected to the PCB via I/O pins. At present, two kinds of secondary sensors are tested for the parking detection purpose in the

perspectives of both reliability and sustainability. In the following sub-section, three sensors are discussed firstly. Then control module, power module and communication module are introduced sequentially.

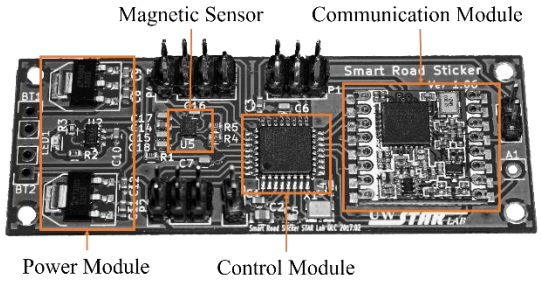

Figure 3.3 PCB of SRS

3.2.1 *Sensor Module – Magnetic Sensor*

The magnetic sensor is one of the most common sensors in many fields including vehicle detection. Its operating principle is detecting the Lorentz force. The magnetic field change will trigger the change of the Lorentz force which can be measured electronically. The fundamental idea of using this kind of sensor is that the magnetic field near this sensor will change when vehicles pass by or run over it. There are several advantages of magnetic sensor: small size, high sensitivity, and low power consumption.

1) Small Size

The magnetic sensor is small when compared to other vehicle detection sensors. Take the sensor MAG3110 which is used in this paper as an example. The actual dimension is $2 \times 2 \times 0.85$mm. Comparably, the light sensor TSL2591 has the dimension of $2.4 \times 2 \times 0.7$mm. And the ultrasonic sensor or video sensor has a much bigger dimension, which is not in order of magnitude. Although the magnetic and light sensor have a similar dimension, the light sensor requires to receive the

environmental light, which means there is no obstacle in front of it to block the light. But there are always dusts or other sundries on top of case, which may influence its performance.

2) High Sensitivity

The second advantage is its sensitivity. The magnetic sensor is not a positive sensor which only receives information and is triggered by outside condition change (i.e. magnetic field). Most modern vehicles contain metals no matter it is paramagnetic or ferromagnetic substance. The existence of vehicles thus will influence their current magnetic field and this influence could be observed through magnetic sensor easily. The MAG3110 sensor has the sensitivity of $0.1\mu T$ while the magnetic strength of the earth is $45\mu T$ [74] and the magnetic change caused by the vehicle is greater than $30\mu T$ [75]. In addition to sensitivity, the maximum sample rate of MAG3110 is $1{,}280Hz$ while the output data rate is up to $80Hz$ with the over sample ratio of 16. Therefore, the magnetic sensor is capable of detecting moving vehicles.

3) Low Power Consumption

For a vehicle detector, especially on-road detector, the power supply is a critical issue for there is almost no external power source. Therefore, power consumption is an essential spec for all detectors. Within a detector, two parts consume the most power, which are sensor and communication modules. The power consumption of the magnetic sensor is very low in microampere level. The supply current of MAG3110 in standby mode is only $2\mu A$ where the sensor is for the most of tithe me. If it is in the active mode, the supply current varies from $8.6\mu A$ to $900\mu A$ depended on the sampling rate. When the sampling rate is $1{,}280Hz$ which is the maximum rate, the supply current is $900\mu A$. When the sampling rate reaches the minimum rate of

$80Hz$, the supply current is $8.6\mu A$. The sampling depends on the specific application. For example, the parking application does not require high sampling a rate, because the vehicle speed is relatively low. Thus, the power consumption can be very low for the whole detection process.

Table 3.1 MAG3110 Tech Specs

Supply Voltage	$1.95V$ to $3.6V$
Dimension	$2 \times 2 \times 0.85mm$
Full-scale Range	$\pm 1000\mu T$
Sensitivity	$0.1\mu T$
Noise (RMS*)	$0.5\mu T$
Working Temperature	$-40℃$ to $85℃$

*RMS: Root Mean Square

Just as described above, the magnetic sensor chosen for the SRS is MAG3110, which is a small, low-power, digital 3-axis magnetometer. Its features are shown in Table 3.1. It uses the I2C serial interface for communication between sensor and CPU.

3.2.2 *Sensor Module – Light Sensor*

The light sensor will output the analog voltage which is linearly related to light strength received. Higher illuminance will generate higher voltage. Based on the light frequency, the environmental light can be categorized into three groups – ultraviolet light, visible light and infrared light. In this application, both the visible light and infrared light are considered comprehensively. Similar to the magnetic sensor, the light sensor is a passive detector which converts the light energy into an analog output. It has advantages of low costs, low power consumption, small dimension. But its disadvantages are also obvious because it is easily influenced by the surrounding environment

which determines that it works as the assisting sensor for verification. Based on the conversion principle, the light sensor can be divided into the following three categories.

1) Phototube Cells

The Phototube cells operate following the photoelectric effect: "*Incoming photons strike a photocathode, knocking electrons out of its surface, which are attracted to an anode. Thus, current is dependent on the frequency and intensity of incoming photons*" [76]. Therefore, the output is in proportion to both the light frequency and strength.

2) Photovoltaic Cells

The photovoltaic cells utilize semiconducting materials that exhibit the photovoltaic effect. The photovoltaic effect is closely related to the photoelectric effect. The main difference is that the photoelectric effect describes that the electron is ejected out of the material, but the photovoltaic effect is used when the excited charge carrier is still contained within the material. The energy generated is in proportion to the light energy received. The most common photovoltaic material is Selenium used in the solar cells.

3) Photoconductive Cells

The photoconductive cells are using the phenomenon that some semiconductor that becomes more electrically conductive because of the absorption of electromagnetic radiation like visible light [77]. Compared to the phototube cells, the photoconductive cells have smaller size. And they are more sensitive when comparing with the photovoltaic cell. The most typical photoconductive cell is the Light-Dependent Resistor (LDR), which is adopted as the light sensor in the SRS.

At first, the photovoltaic cells are selected as the light sensor as well as the power generator at the same time. The photovoltaic cell panel's dimension is $60 \times 60 \times 3mm$. And its maximum output voltage is $5.5V$. However, the actual performance is not as good as expectation. There are two disadvantages when applying the photovoltaic cells. The first one is low precision and narrow detection range when not considering the rear stage load. The photovoltaic cells are almost used for the power generation, its function is not measuring the light intensity. The second one is that the load of rear stage will influence the output because of the internal resistance in the photovoltaic cells. Under the condition of consistent light, the greater the load current is, the lower output voltage of the photovoltaic cells is.

In order to improve the performance of the light sensor, the solar panel is replaced by a high-dynamic range photoconductive cell whose responsibility is only measuring the light intensity. The model is TSL2591, whose dynamic range is $600{,}000{,}000{:}\,1$, and it can detect illuminance ranging from $188\mu Lux$ to $88{,}000Lux$. This impressive detection range is achieved by using different gains. For example, the detection scale is from $1.34Lux$ to $88{,}000Lux$ with gain of 1. The scale will become $0.003 \sim 205$Lux when the gain is 428. What's more, this sensor contains both infrared and full spectrum diodes. Thus, it has the ability to measure infrared, full-spectrum or human-visible light separately. Considering this is also a passive detector, this light sensor is energy-saving with operating current of $400\mu A$ in active mode and $5\mu A$ in power-down mode. It uses I2C serial interface for communication which is the same as the MAG3110, which simplifies the communication structure.

3.2.3 *Sensor Module – Ultrasonic Sensor*

The ultrasonic sensor is used to measure the distance between the SRS and the vehicle bottom. It has two functional parts – transmitter and receiver. The transmitter converts the electrical signals into ultrasound, and then receivers convert the ultrasound reflected from the object into electrical signals. With the development of sensor technologies, the transmitter and receiver are integrated into one transceiver with smaller size. It has the ability to send and receive ultrasound using the same probe. There are three advantages to use the ultrasonic sensor as the detector.

1) Unaffected by Target's Materials

The operating principle decides that the ultrasonic sensor is almost not influenced by the target's materials no matter whether it is metal or transparent. The only exception is the material absorbing the ultrasound. In this regard, it is better than the magnetic sensor and light sensor. The magnetic sensor requires that the target's material can distort the nearby magnetic field, and the light sensor has the requirement for target's color and transparency.

2) Unaffected by Environmental Light or Dust

The ultrasonic sensor uses ultrasound to detect objects. It is not influenced by environmental light totally. However, dusts in the air have a little impact because heavy dusts will hinder the ultrasound in some extreme situations. And heavy dusts may also influence the operation of the probe by limiting its vibration. Comparably, the light sensor will suffer the challenge of environmental light and dusts. The magnetic sensor has no concern about this challenge.

3) Provision of Depth Information

The last advantage over the two other sensors is providing the depth information which is a direct measurement for vehicle detection. Both magnetic sensor and light sensor outputs the indirect measurement like magnetic field strength or illuminance, which is not corresponding to whether there is a vehicle above the detector directly. The detection algorithm of transforming the indirect output to occupancy status is very important and may generate extra detection errors, while the ultrasonic sensor does not have this problem since there is no intermediate transformation.

Although the ultrasonic sensor has some unique advantages that the two other sensors do not have, there are still some drawbacks to be addressed. And these drawbacks limit its application in the on-ground vehicle detector. These drawbacks are mainly concluded in three perspectives which are list below.

1) High Power Consumption

The ultrasonic sensor belongs to the active detector which sends out and receives the ultrasound. And this self-transmission process consumes much power. For example, the operating current of the most common non-waterproof ultrasonic sensor HC-SR04 is $15mA$, while its standby current is still more than $1mA$. In this application, the waterproof ultrasonic sensor has the measurement current of $40mA$. And its standby current is about $5mA$. In order to save energy, the power supply will be cut off when the ultrasonic sensor does not work, and its current can drop down to almost zero. Another way is reducing its detection frequency. Therefore, the ultrasonic sensor is designed to verify the detection results of magnetic sensor.

2) Weak Water-proof Ability

Considering that the ultrasonic probe cannot be placed under the top of the case, the probe is thus exposed to the outside. The waterproof becomes an important issue for both the ultrasonic sensor and other electronic components, because the raindrops or vapor may get inside along the gap between the probe and case. There are two requirements for the waterproof. Firstly, the ultrasonic probe itself must be waterproof. Secondly, the gap between the probe and case should be fully sealed using epoxy or other fillers.

3) Large Dimension

Compared to two other sensors, the dimension of ultrasonic sensor is greater than two others. Thus, the large dimension is one of reasons that the ultrasonic sensor is not integrated into the PCB. Another reason is the placement inside the SRS. It is closer to the top of the case in order that the probe can reach out. But that area does not have enough space to accommodate the PCB. With the same battery capacity and similar component layout, the overall dimension of SRS Version Two dimension is thus limited and cannot make it as small as SRS Version One.

The basic tech specs of the waterproof ultrasonic sensor are shown in Table 3.2. The lower bound of the supply voltage is $3.3.V$, which is the same as the operation voltage. The peak current is $30mA$ and is also greater than the output capability of CPU's digital pins. Therefore, it is directly connected to the regulator. And the maximum output of the regulator should be high enough. It can be seen that the working range is from $25cm$ to $400cm$ which covers the ground clearance of most vehicles.

Table 3.2 Waterproof Ultrasonic Sensor Tech Specs

Supply Voltage	$3.3V$ to $5V$
Peak Current	$30mA$
Dimension	$41 \times 29 \times 20mm$
Working Range	$20cm$ to $400cm$
Sensitivity	$0.3cm$
Working Current	$40mA$
Working Temperature	$-10℃$ to $70℃$

3.2.4 *Control Module*

The control module is the core of controlling different modules and processing data. It will trigger sensors for detection, receive sensor data, compute detection results and finally transmit results to base station through the communication module.

Initially, the SRS is built on Arduino platform. The Arduino is one of the most popular open-source electronics platforms on hardware and software development for all level users. It provides an easy interface to interact with hardware through Arduino programming language. Thus, the ATmega328P 8-bit microcontroller was used since it is also the most popular CPU for Arduino boards. And most importantly, there are many 3rd-party libraries to support different sensors and to achieve various functions. The basic technical specs of ATmega328P are shown in Table 3.3.

The power consumption greatly depends on supply voltage and operation frequency. When it is working at $1MHz$ and $1.8V$, its supply current at active mode is $200\mu A$ and at standby mode is $0.75\mu A$. The lower the frequency and supply voltage is, the less power it will consume. However, this is the minimum power consumption for this CPU. Considering the voltage matching of all sensors and communication module, the CPU has to work at $3.3V$. If the CPU and sensors work at different voltages, more regulators and logic convertors will be added, which increases the

complexity of the circuit and reduces the robust of system as well. As a result, the active current at operation frequency of $1MHz$ and supply voltage of $3.3V$ is about $600\mu A$ and the standby supply current is $180\mu A$. This CPU performs an important role in testing and verifying the basic idea of the SRS on our preliminary stage.

After finding the ATmega328P cannot meet the power-efficiency demand, it is replaced by MSP430 which is specially designed for signal control and has the ultra-low power consumption. When MSP430 is working at operation frequency of $1MHz$ and supply voltage of $3.3V$, its active current is $330\mu A$ and its standby supply current is $80\mu A$. The average current is less than half of the previous ATmega328P, which means its service life extends more than one time with the same battery. The basic tech specs of MSP430 are shown in the Table 3.4.

Table 3.3 ATmega328P Tech Specs

Supply Voltage	$1.8V$ to $5.5V$
I/O	28 programmable I/O lines
Working Speed	$0.1MHz$ to $16MHz$
Working Temperature	$-40℃$ to $85℃$

Table 3.4 MSP430 Tech Specs

Supply Voltage	$2.0V$ to $3.6V$
I/O	24 programmable I/O lines
Working Speed	$1MHz$ to $16MHz$
Working Temperature	$-40℃$ to $85℃$

3.2.5 *Power Module*

The power module provides the power supply for the whole system. The power module has two parts – power source and power management. There are two power sources in SRS – solar panel

and LiPo battery. The solar panel is the power generator and the LiPo battery is the power storage. The solar panel and LiPo battery are connected through a step-down regulator and a battery charger management controller. This step-down regulator will output a stabilized voltage for the battery charger management controller from the the solar panel. And the battery charger management controller is responsible for charging the battery and supplying the system when there is enough environmental light. When the light becomes weak and is not enough to support the system, the battery will supply the system operation. Considering that the normal output voltage of the battery is 3.7V and the voltage of the subsequent circuit is 3.3V. Therefore, another step-down regulator with output of 3.3V is necessary to provide a stable power supply. The schematic diagram of the power module is shown in Figure 3.4.

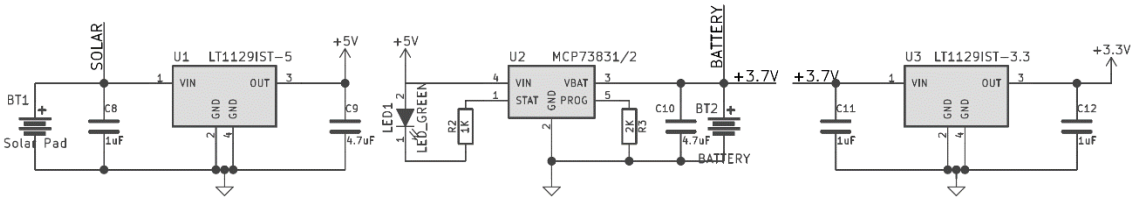

Figure 3.4 Schematic Diagram of Power Module

The dimension of the solar is $60 \times 60 \times 3mm$ and its maximum output voltage is $5.5V$ and the current is $100mA$. The average supply current of the SRS is less than $0.7mA$ and its peak current is $130mA$. In average, the power consumption of one day can be compensated by the solar-panel full charge of 0.17 hour. The peak current appears when the SRS sends detection results to the nearby station. At this moment, both solar panel and battery provide the supply to the system. The LiPo battery capacity is $6{,}000mAh$ which will support the system operation for more than one year without any solar charge. The capacity is chosen for two reasons. The first reason is the dimension limit. In order to place the SRS above the ground, the dimension should be as small as

possible. This capacity is the trade-off between the small dimension and long battery life. The second reason is that the power consumption is low, and this capacity is sufficient for all work. In addition, higher capacity indicates higher costs.

3.2.6 *Communication Module*

The communication module receives the detection results from the control module and then sends them to nearby base stations. Considering the scalability and low power-consumption of the SRS, there are several communication protocols satisfying these demands, which are BLE, ZigBee and LoRa. Bluetooth is designed for short-range communication and continuous, streaming data applications. And BLE, which is also called as Bluetooth 4.0, consumes much less power than its previous version, and does not exchange as much data as before. BLE works on $2.4GHz$ and its sensitivity is about $-93dBm$. Both classic Bluetooth and BLE are using scatternet structure. The comparison between Bluetooth classics and BLE is shown in Table 3.5.

Table 3.5 Comparison between Bluetooth Classics and BLE

	Bluetooth Classics	BLE
Communication Distance	$100m$	$> 100m$
Air Data Rate	$1Mbps$ to $3Mbps$	$0.125Mbps$ to $1Mbps$
Latency	$100ms$	$6ms$
Power Consumption	$1W$	$0.01W$ *to* $0.5W$
Peak Current	$30mA$	$15mA$

ZigBee is a mesh network protocol which is designed to carry small amount of data. Similarly, both ZigBee and BLE are working on the same Industrial, Scientific and Medical (ISM) band of $2.4GHz$. Different from the scatter network, the data from a one node travels on a web of nodes

until the transmission gets to the gateway. This topology extends its coverage from the radius of $100m$ to a much larger area. In addition, the ZigBee has a stronger TX power and better sensitivity ($-102dBm$) which contributes to the better communication quality and longer distance (about $300m$) if there are only two nodes in the network. However, the practical communication distance will be shorter than $300m$. There are always some $2.4GHz$ wireless devices inside the parking facilities to interfere the communication distance. And the building will also have negative impacts on the communication quality.

Therefore, a communication protocol with a long communication-distance and a low-power consumption is needed for the SRS. LoRa is exactly that a protocol for this application. There are two standing features of LoRa compared to BLE and ZigBee. The first one is the super long communication-distance of more than $2000m$ in the open area, which is 20 times than BLE and 6 times than ZigBee. The second one is the large node capacity of more than 200 nodes. The communication frequency is $915MHz$ in SRS. Thus, the antenna length should be $78mm$ which is equal to one quarter of the wavelength, to maximize the transmission distance.

The LoRa chip version adopted for SRS is RFM95W, and its techical specs are shown in the Table 3.6. According Table 3.6, it can be seen that the supply voltage range of RFM95W covers the SRS supply voltage at $3.3V$. Thus, no extra regulator will be added to the communication module.

The power consumption in different modes is shown in Table 3.7. Although the TX current is high, the communication module will remain in the sleep of idle mode in most periods, which indicates the peak current will not consume much power during the whole battery life, especially compared to the sensor part. One more thing to be addressed is the consideration of great current fluctuation. The maximum current when transmitting data to the base station is thousands of times

than the minimum current during the detection interval. Thus, the capacity is important to be added into different places to filter peak noise which may damage the whole system.

Table 3.6 RFM95W Technical Specs

Supply Voltage	$1.8V$ to $3.7V$
Frequency	$915MHz$
Air Data Rate	$0.3Mbp$
Sensitivity	$-148dBm$
Communication Distance	$> 2000m$

Table 3.7 Power Consumption in Different Modes

Sleep Mode	$0.2\mu A$
Idle Mode	$1.5\mu A$
Standby Mode	$1.6mA$
RX Mode	$11.5mA$
TX Mode ($+7dBm$)	$20mA$
TX Mode ($+20dBm$)	$120mA$

3.3 CASE DESIGN

There are two kinds of cases designed for SRS which are shown in Figure 3.1. The material of SRS is transparent Acrylonitrile Butadiene Styrene (ABS). Figure 3.1 (b) displays that the case is black which is built with polylactide (PLA) material using the 3D printer. The practical material is still transparent ABS. The SRS is placed on the ground directly without any other safety protection, which requires the strong compressive capacity and waterproof ability.

Initially, the case material was zinc alloy to enhance the case strength which was widely used in other road light studs. After several weeks of tests, it was found this metal material will affect the communication distance. In the open area, it was less than 70% of the distance when using the

ABS as the case material. If a vehicle was over the SRS, the distance was shorter due to the signal block of the vehicle body. In consideration of the communication distance, the material was then replaced by ABS.

However, problems of the compressive capacity come with the material change. The ABS itself is not strong enough to resist the rolling of a small vehicle. One solution is adding filler inside the SRS to strengthen the case. After comparing different filler materials in the perspectives of strength and conductivity, the electronic grade potting epoxy resin is used as the filler. There are three reasons for this option. The first reason is good liquidity before solidification and strong compressive capacity after solidification. The second reason is non-conductivity which will not influence the performance of electronic part. The third reason is improvement on the waterproof. All electronic components are wrapped in the epoxy resin and are isolated from all kinds of water. The dimensions of these two kinds of cases are shown in Table 3.10.

Table 3.8 SRS Case Dimension

	SRS Version One	SRS Version Two
Diameter	$150mm$	$135mm$
Height	$38mm$	$30mm$

The first version has a larger dimension due to two perspectives. The first perspective is higher battery volume. The originally designed battery volume is $10{,}000mAh$ which is 60% higher than the current one. Higher volume indicates larger size. During improving process, the system is proven to be power-saving since there is no need to use high volume battery. And the second one thus has a smaller battery compartment. The second one is the inner components layout. The components in the first version are placed vertically, which wastes some space. The second version places components horizontally at the bottom of the SRS except ultrasonic sensor. Considering

that the probe of the ultrasonic sensor should be out of the upper case, this sensor is placed above the PCB. Therefore, the outlook difference mainly lies in that the second version has the hole designed for the ultrasonic sensor.

Chapter 4. SOFTWARE DESIGN

This chapter introduces the detection algorithms for SRS. These algorithms developed in this research have four categories – magnetic detection, light, and ultrasonic detection and fusion algorithms. Different parking modes tested were shown in Figure 4.1.

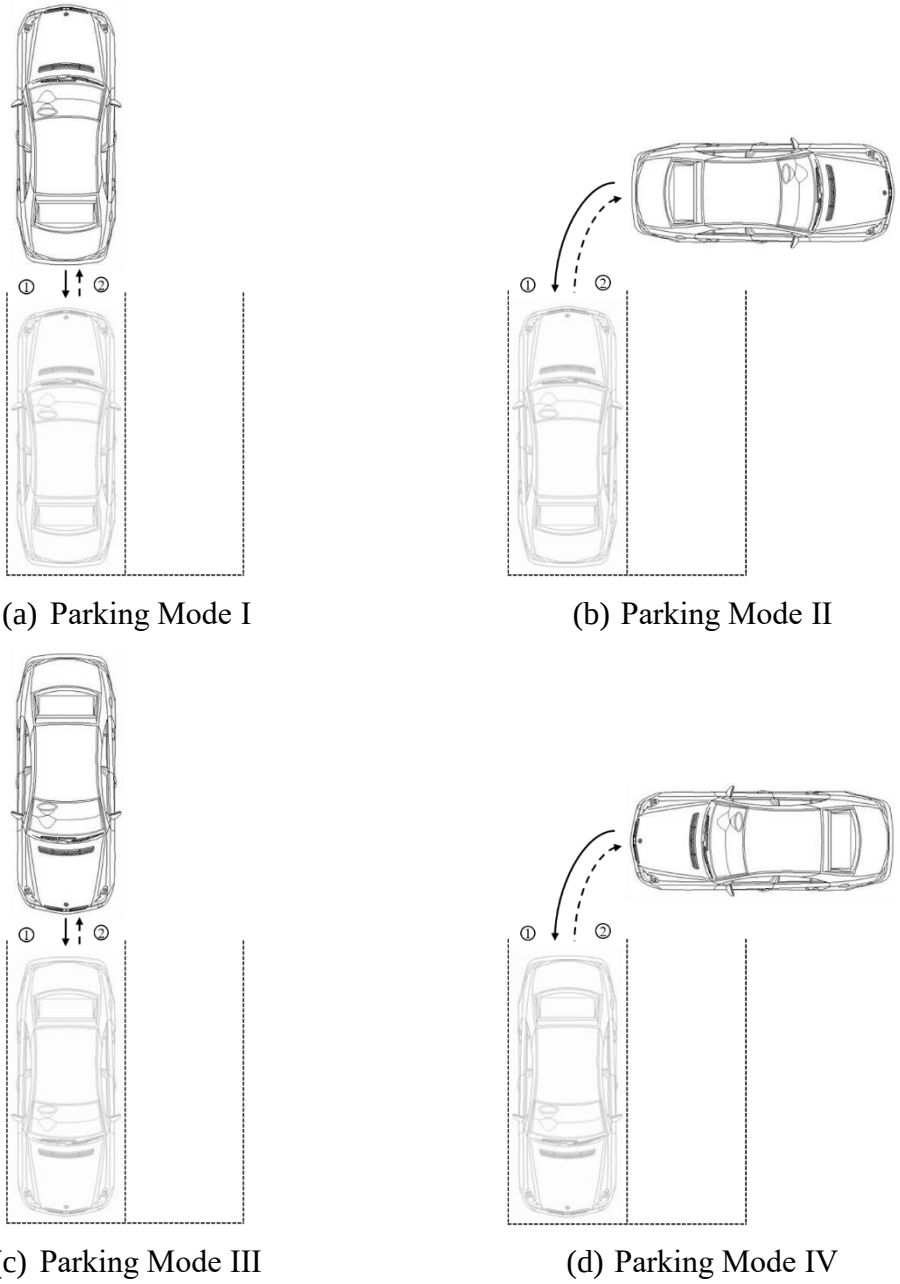

(a) Parking Mode I (b) Parking Mode II

(c) Parking Mode III (d) Parking Mode IV

Figure 4.1 Parking Modes

Each subfigure of Figure 4.1 shows how a vehicle drive in and out of the parking slot. The solid arrow indicates the direction of a vehicle getting in and the dash arrow indicates the direction of a vehicle getting out.

4.1 MAGNETIC SENSOR DETECTION ALGORITHM

The magnetic sensor data was collected in both indoor and outdoor parking garages at University of Washington. The data collecting process is shown in Figure 4.2. The sensor node is placed near the center of the parking slot. The vehicle firstly enters the parking slot and stay over the SRS for several seconds. And then vehicle will follow the original routine to exit the parking slot. One point to be addressed here is that the front or rear axle must go over the SRS to ensure the magnetic sensor can detect the magnetic field distortion. In Figure 4.2, the x-axis is defined as the direction which is the same as the parking slot's direction. And the y-axis is thus defined as the direction which is vertical to the parking slot's direction. The z-axis is upward direction from the ground.

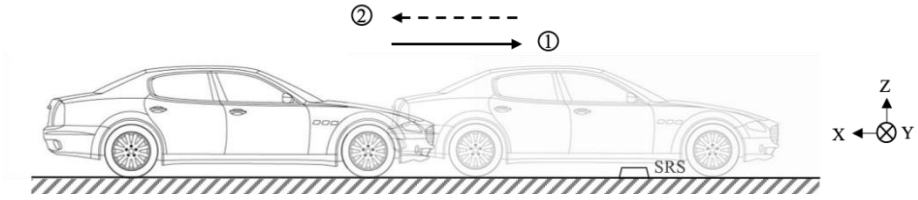

Figure 4.2 Sensor Test Process

One set of sample output data of the magnetic sensor is shown in Figure 4.3. The test scenario describes an entering process. Part (a) – (c) indicates the magnetic field value of x, y and z-axes. The horizontal axis is the process time with unit of second, and the vertical axis is the magnitude.

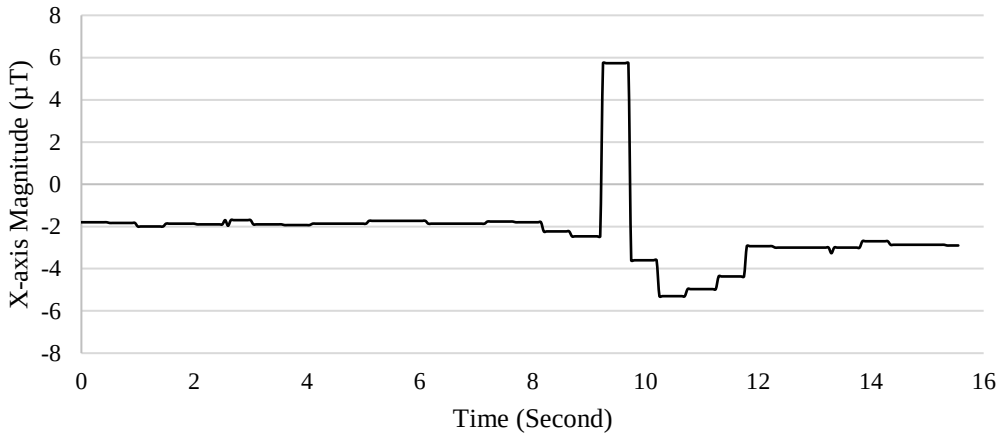

(a) X-axis Magnetic Field Distortion

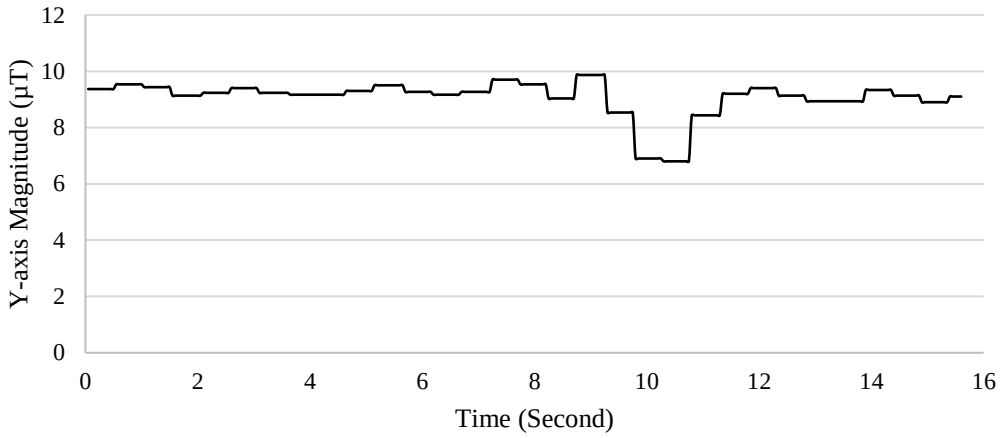

(b) Y-axis Magnetic Field Distortion

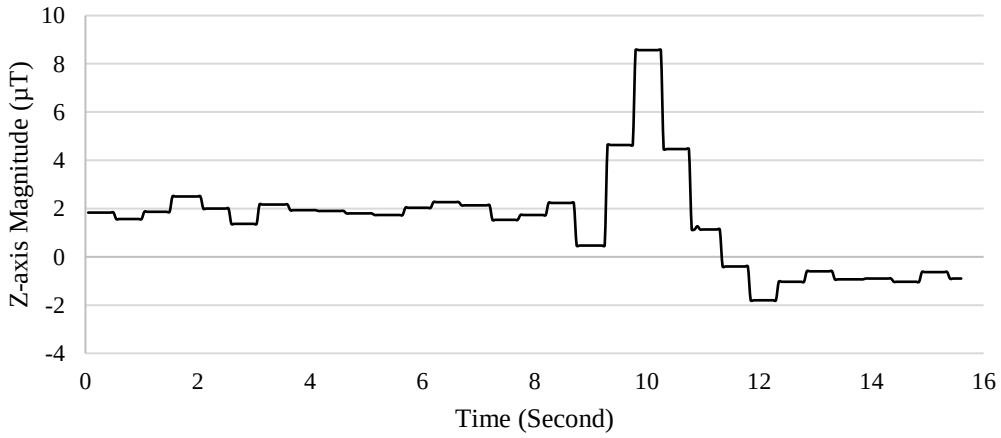

(c) Z-axis Magnetic Field Distortion

Figure 4.3 Magnetic Sensor Output

According to Figure 4.3, the vehicle can significantly affect the magnetic field but has various influences on three dimensions. The impacts on x and z-axes are comparably greater than the y-axis. The magnetic field change on the x-axis and z-axis is used to describe the occupancy status change. What's more, different positions of a vehicle also have different impacts. Positions near the front and rear axles, where ferromagnetic materials concentrate, have greater impacts, while the middle position hardly influences the magnetic field on x-axis and z-axis.

This paper uses the magnetic field on z-axis as the magnetic sensor output. Compared to the magnetic field distortion on x-axis, the magnetic field distortion on z-axis has similar change but has a more stable output performance. The output on both x and y-axes greatly depends on two perspectives – sensor's positive direction and vehicle's direction. When the sensor's x-axis has the same or opposite direction as the parking slot, the magnetic field change reaches the maximum. If their directions have an angle which is not 0 or 180 degrees under the assumption that the vehicle will enter or exit straightly, the range of the change will decrease dramatically. And this feature requires that the SRS should be installed properly by making it toward the right direction. However, it is hard to guarantee during the installation process since it is not easy to distinguish the positive direction. The second perspective is the vehicle's direction. Even if the SRS is installed correctly and accurately, the vehicle does not enter the slot straightly which may weaken the change of the magnetic field. Based on the analysis above, the z-axis is chosen as the detection direction. The detection algorithm of the magnetic sensor can be divided into four parts – smoothing, wavelet transformation, variation computation, and threshold comparison. The detection process is shown in Figure 4.4. The $X[n]$ is the data packet used for wavelet transform. The length of each data packet N is 10, which means it contains 10 sample points with detection interval $1/f$. $D[n]$ is the data packet after the smoothing operation whose function is reducing the sample noise. $W[n]$ is

the result of the wavelet transform whose length is half of the input data packet length and is $N/2$. $cA[n]$ is the approximate coefficient of $W[n]$ and V_1 is the variance of $cA[n]$. T_1 and T_2 are thresholds for variance and time interval to check whether two changes are too close respectively.

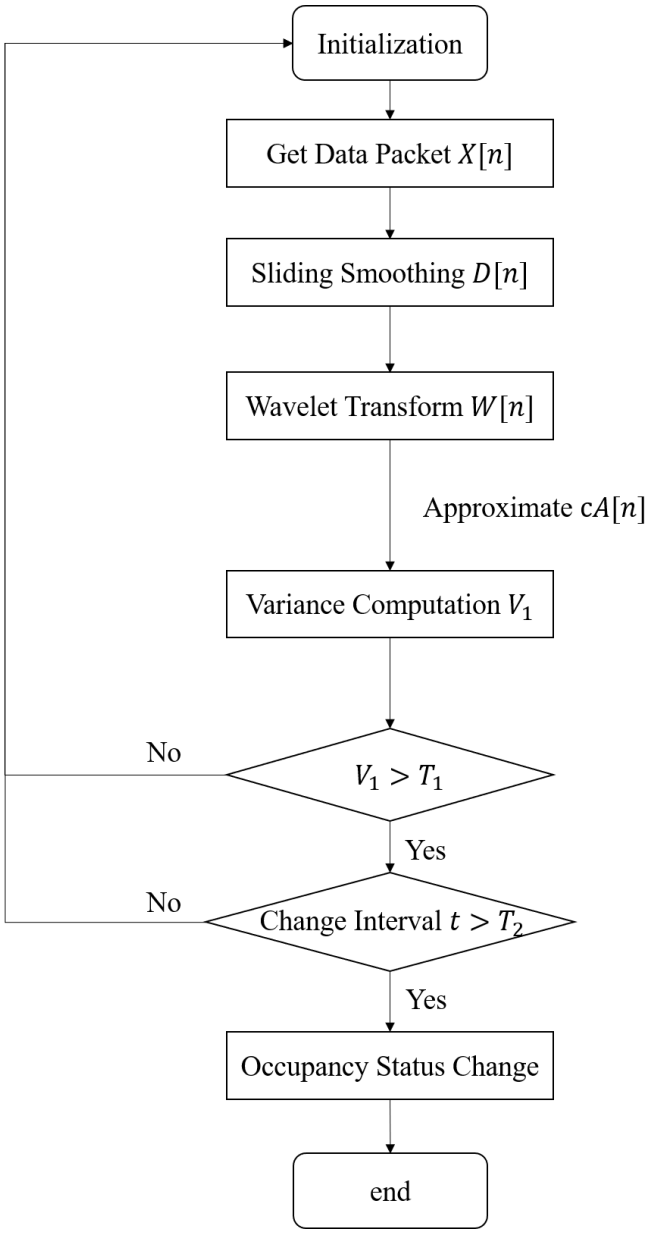

Figure 4.4 Magnetic Sensor Detection Algorithm

4.1.1 *Smoothing*

The smoothing method is the moving average method whose basic idea is computing the average of nearby sample points and its function is shown in Equation (4-1).

$$D[n] = (X[n-m+1] + \cdots + X[n])/m \quad (4\text{-}1)$$

where m is the average length and $n > m$. For $D[n]$ $(n \leq m)$, no smoothing operation will be taken. In this paper, the m is set as 3.

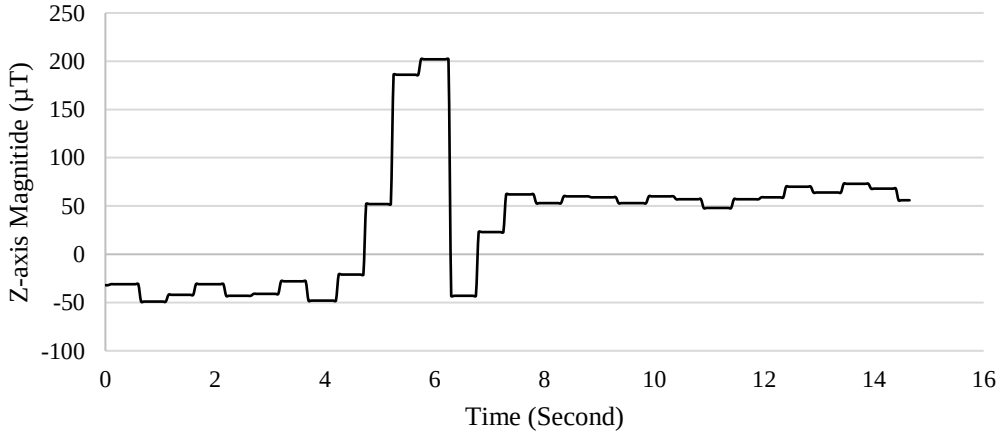

(a) Sample Data before Smoothing

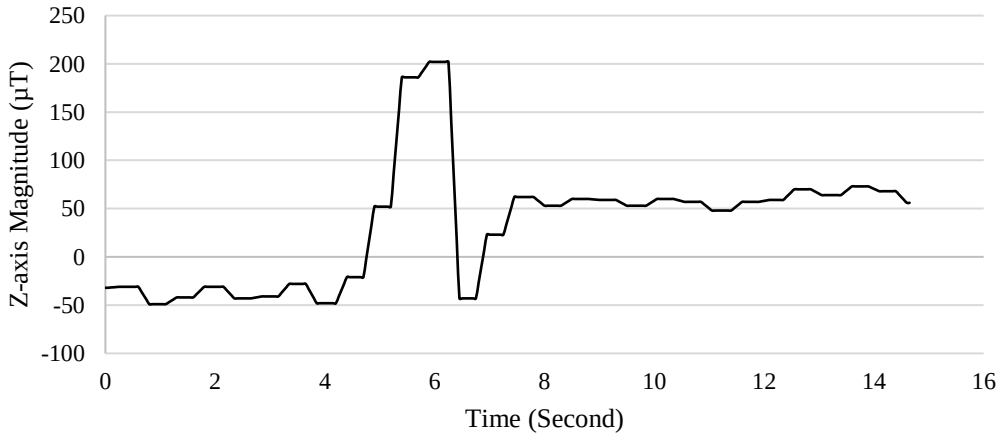

(b) Sample Data after Smoothing

Figure 4.5 Sample Data of Smoothing Process

In order to clarify the results of smoothing more clearly, the results shown in Figure 4.5 are taken on longer data packets whose length are greater than designed packet length. In Figure 4.5, the average length is chosen as 3. Through this process, the noise will be reduced, and the transition becomes smoother.

4.1.2 *Wavelet Transform*

The wavelet transform is the most important step in the magnetic detection process, which would decompose the raw input data into two parts – approximate and detailed coefficients. This paper uses discrete wavelet transformation (DWT) because all input data is discrete sample points.

The Fourier transform is widely used to analyze the signal feature in the frequency domain. But it still suffers some drawbacks when facing unstable signals. And in most cases, the signals in the natural world is unstable. If the frequency changes with time, it is difficult to analyze the signal in the frequency domain. In order to solve this problem, another method called short-time Fourier transform (STFT) is put forward which divides the signal in time domain into several segments with equal length.

The one-level DWT of the input signal $D[n]$ is shown in Figure 4.6. The input signal is decomposed simultaneously using a low-pass filter $l[n]$ and a high-pass filter $h[n]$. However, the magnetic field distortion caused by vehicles does not contain much high-frequency information. This paper only uses the low-pass filter to get the approximate coefficients $cA[n]$. The equation to compute the coefficients is shown in Equation 4-2, which includes a convolution operation on input data using the impulse response $l[n]$ and a sub-sampling operation. The operator $\downarrow$ is the downsample operator. The expression of $l[n]$ is shown in Equation 4-3.

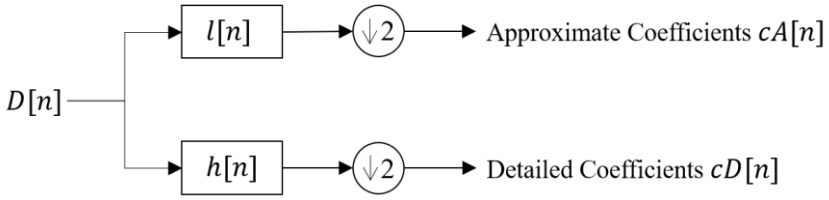

Figure 4.6 DWT Process

$$cA[n] = (D \downarrow l)[n] = \sum_{k=1}^{2} D[k]l[2n-k] \tag{4-2}$$

$$l[n] = \begin{cases} -0.7071, n = 1 \\ 0.7071, n = 2 \end{cases} \tag{4-3}$$

4.1.3 *Variance Computation and Comparison*

After getting the approximate coefficients in the previous step, the variance of coefficients V_1 is then computed to describe the magnetic field change during this period. The high variance means there is a great magnetic field distortion which is caused by the occupancy status change. The variance function is shown in Equation (4-4) where μ is the mean value of coefficients. The expression of μ is shown in Equation (4-5).

$$V_1 = \frac{1}{n}\sum_{i=1}^{n}(cA[i] - \mu)^2 \tag{4-4}$$

$$\mu = \frac{1}{n}\sum_{i=1}^{n} cA[i] \tag{4-5}$$

The variance changes when a vehicle enters and leaves a parking slot in parking way III are shown in Figure 4.7. Both part (a) and part (b) shows that the front vehicle axle can cause great magnetic field change when it passes over the magnetic sensor. Therefore, the threshold T_1 can be

applied to distinguish whether there is a vehicle passing over the SRS. However, there are still some drawbacks which cannot be solved by a single magnetic sensor. The first problem is the magnetic sensor can only detect the change of occupancy status but cannot detect whether the parking status is occupied or empty. The main reason is that the magnetic field can either be weakened or strengthened when a vehicle is over the SRS.

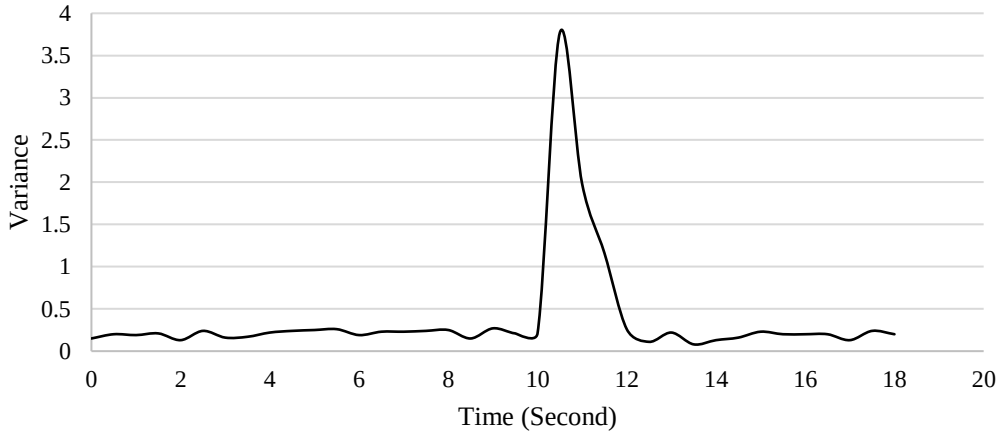

(a) Variance Change when a Vehicle Enters

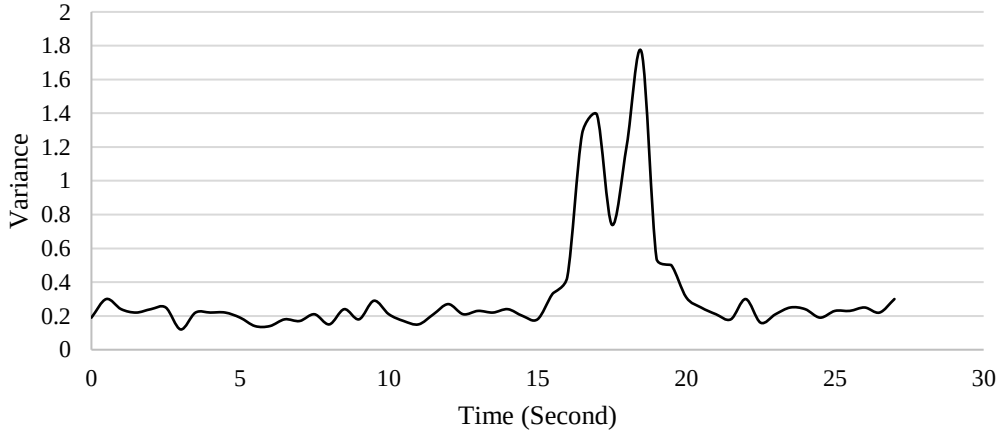

(b) Variance Change when a Vehicle Leaves

Figure 4.7 Variance Change when a Vehicle Enters and Leaves

The second problem can be observed in Figure 4.7 (b) that multiple peaks may appear during this process. If a vehicle just passes by the SRS rather than parks, the variance peaks cannot be

distinguished. It is hard to tell which axle these peaks belong to. The third problem is the occupancy status may be opposite to the real when one change is missed. And this error cannot be corrected without external support. In summary, it is important to make use of other sensor(s) to solve these problems, which will be discussed in the following sections.

4.2 LIGHT SENSOR DETECTION ALGORITHM

The light sensor is an important assistance to the magnetic sensor since it will output lower value if it is occluded by a vehicle. The occupancy status will be thus confused. Multiple tests have been done at different time. There are two kinds of light received by this sensor – visible light and infrared light. They have different properties and performance. The infrared light is more sensitive to the heat change while the visible light is more sensitive to the environmental light change. The visible light output is defined as $L_v[n]$ and the infrared light output is defined as $L_i[n]$. In order to get the maximum value change, the overall change $L[n]$ is the summation of $L_r[n]$ and $L_i[n]$, whose expression is shown in Equation (4-6).

$$L[n] = L_v[n] + L_i[n] \tag{4-6}$$

The sample rate of the light sensor is $10Hz$ and gain is 25 which suits the most outdoor environment. The sensing range is from $0.05Lux$ to $3520Lux$. The light sensor output is shown in Figure 4.8 including both daytime and night tests. Figure 4.8 (a) shows the sensor output during the daytime. The actual illuminance was much higher than $3520Lux$ and reached its maximum scale when it is not occupied. When the vehicle was on top of the SRS, the illuminance strength dropped down about 60%. This test shows that the even though the vehicle would raise significant illuminance change when covering the SRS. Figure 4.8 (b) shows the data in night test. The basic

illuminance was low and was even about $10Lux$ when there was nothing occupying. The illuminance would drop to $0.2Lux$ when the sensor node was occupied. The illuminance in occupied condition is less than 2% of original illuminance. According to these two sets of test data, it can be observed that the occupancy of a vehicle can have significant impacts on the light strength received by the light sensor.

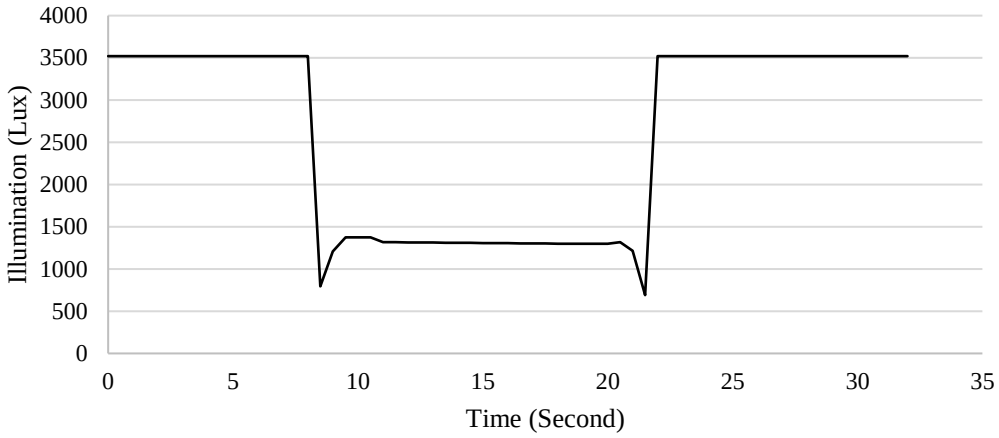

(a) Light Sensor Output at Daytime

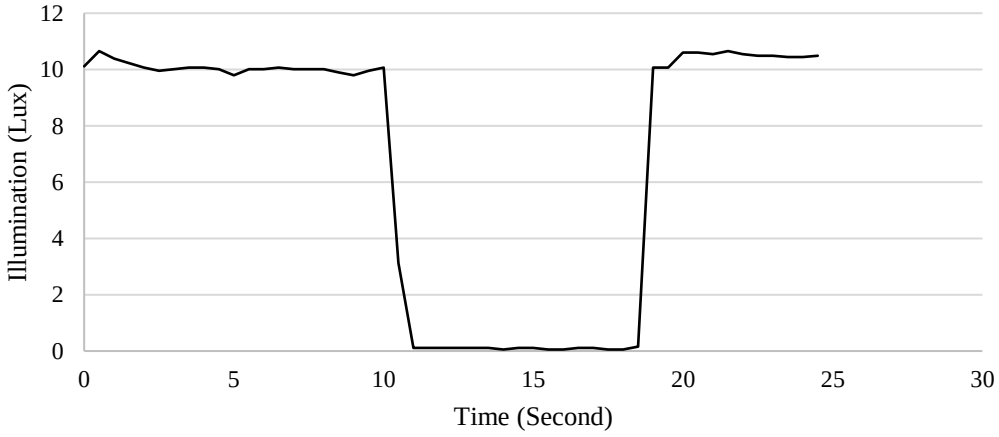

(b) Light Sensor Output at Night

Figure 4.8 Light Sensor Output at Daytime and Night

Another important factor influencing the detection results is the sensor's gain which limits the

detection scale. Lower gain is suitable for the brighter environment while higher gain is suitable for the darker environment. The natural light in the open area is not stable and has great variance during a day when comparing to the light in garage. If the gain is as high as 100. The maximum illuminance detected is $800Lux$ which is even lower than the illuminance under the vehicle shown in Figure 4.8 (a). As a result, this sensor cannot detect the occupancy change when the environment light is bright. If the gain is as low as 1, the detection scale becomes $1.3Lux$ to $88{,}000Lux$ with precision of $1.3Lux$. In the dark environment, the illuminance can be only $10Lux$ without any occupancy, which is shown in Figure 4.8 (b). It is hard to distinguish the cause of the light change since the noise may contribute similar effects. Therefore, the gain value is also important for the detection results.

Table 4.1 Illuminance Levels [78]

Condition	Illuminance (Lux)
Full daylight	10,000 ~ 25,000
Overcast day	1,000
Very dark overcast day	100
Twilight	10

Paul Schlyter's work [78] analyzed some typical illumination levels which are listed in Table 4.1. According to Table 4.1, the detection scale covers most scenarios with the gain of 25. Although, the sensor output will saturate under the condition of full daylight since the maximum illuminance detected is $3{,}520Lux$, the illuminance under the vehicle can be considered as the condition of overcast day whose illuminance is $1{,}000Lux$. There is still a significant difference between the overcast-day illuminance and maximum illuminance detected. Even under the condition of twilight, the change can be detected.

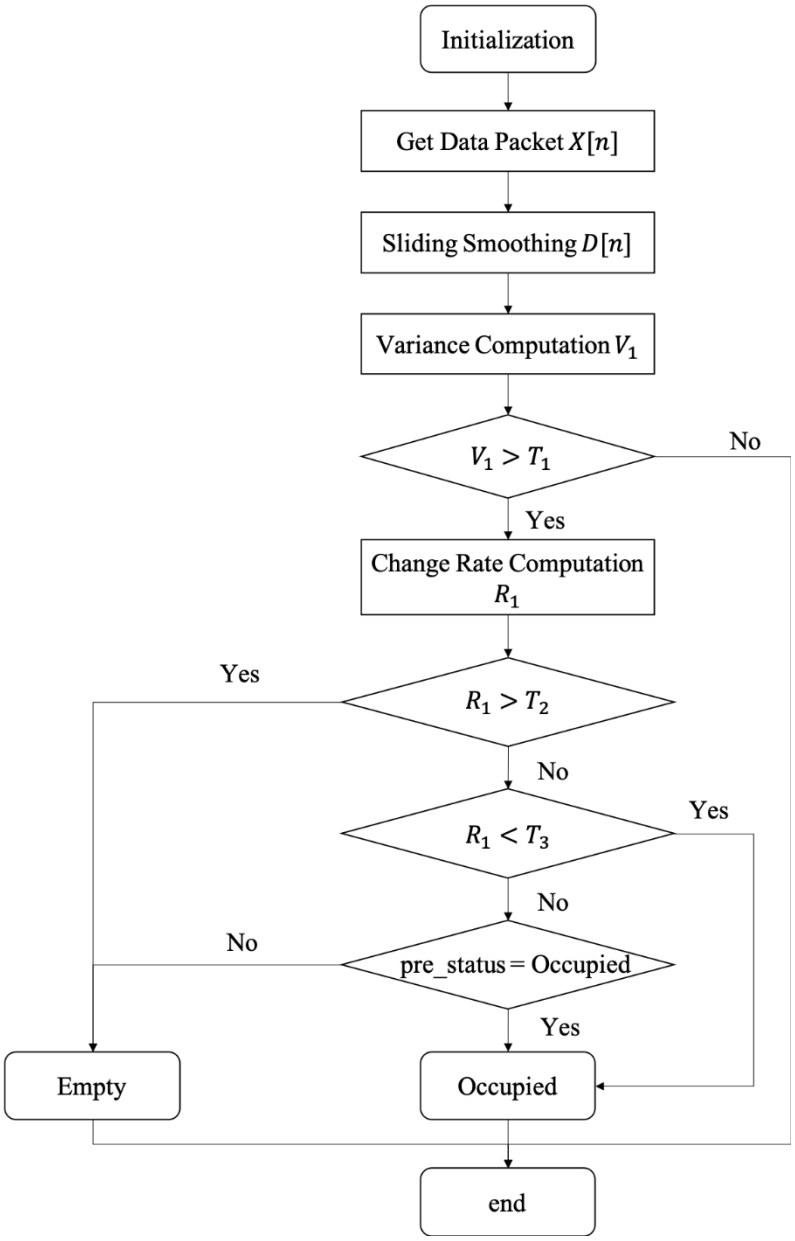

Figure 4.9 Light Sensor Detection Algorithm

The detection algorithm framework is shown in Figure 4.9. The basic idea is analyzing the data variance and the change rate. The data variance will indicate whether there is a light change, and the change rate will indicate the light change direction. Instead of comparing two adjacent points, this algorithm analyzes a data packet containing a series of data with a specific length N. And its detection frequency is $5Hz$.

4.2.1 *Smoothing*

After collecting a data packet, the sliding smoothing operation is taken to reduce the noise. In most scenarios, the illumination is stable when its occupancy status is decided. Although the natural light may change, its change speed is low which does not raise great variance change. However, the artificial light may flash intermittently and has the similar frequency as the alternating current which is 60Hz in the United States because of illumination principle. One set of light sensor data with environmental light flashing is shown in Figure 4.10.

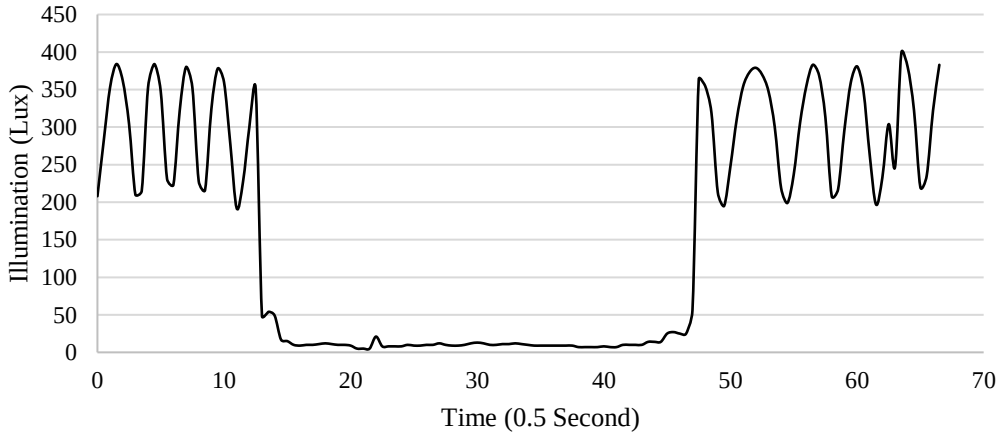

(a) Light Sensor Output before Filtering

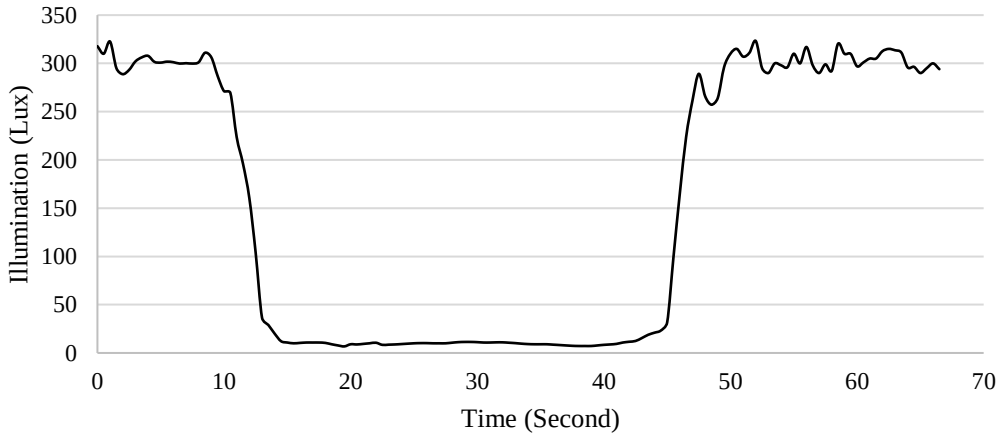

(b) Light Sensor Output after Filtering

Figure 4.10 Light Sensor Output with Light Flashing

The light strobe will lead the inconstant output of the light sensor which is shown in Figure 4.10 (a). Considering the thermal inertia, the illuminance does not drop down to zero but still have significant fluctuation. To reduce the effects of this phenomenon, the sliding smoothing filtering is applied to process the light sensor output. The filtering function is shown in Equation (4-7) whose sliding window size is L. The $D[n]$ is the filtered results, and $X(n-k)$ is the sensor output at five consecutive times respectively, where k is from 0 to 4. Figure 4.10 (b) shows the output after filtering fluctuation caused by light flashing. The output is much smoother than the input.

$$D[n] = \frac{1}{L}\sum_{k=0}^{L-1} X[n-k] \tag{4-7}$$

4.2.2 *Variance Computation and Comparison*

After smoothing the input data, the variance of smoothed illuminance data V_1 is computed using Equation (4-8), where μ is the mean value of D. The expression of μ is shown in Equation (4-9). If the variance is greater than the threshold T_1, it indicates there is a significant light change and it will go to the next step of computing the illuminance change rate. Considering the variance is highly related to the absolute value of illuminance, the variance threshold T_1 based on the current illuminance. Therefore, this threshold is adaptive whose expression is shown in Equation (4-10), where ρ is the global variable to adjust the threshold in all conditions. The threshold is related to both maximum value in data packet D and packet length N. The bigger the maximum value is, the higher the threshold is. And the smaller the data packet length is, the lower the threshold is.

$$V_1 = \frac{1}{N}\sum_{n=1}^{N} (D[n]-\mu)^2 \tag{4-8}$$

$$\mu = \frac{1}{N}\sum_{n=1}^{N} D[n] \tag{4-9}$$

$$T_1 = \rho \cdot \frac{\max(D)}{\sqrt{N}} \tag{4-10}$$

The variances of consecutive data packets are shown in Figure 4.11 with a solid line which records the same data shown in Figure 4.8. Figure 4.11 (a) indicates the daytime results and Figure 4.11 (b) indicates the night results. The dotted lines in Figure 4.11 indicates the adaptive threshold. It can be observed that the illuminance change, which is caused by vehicle entering and leaving, leads to great variance changes which can be clearly identified by the adaptive threshold.

When the variance computed in the previous step is higher than the threshold, then the change rate R_1 will be computed. The change rate defined here is used to represent both the change direction and change scale. The variance cannot provide the change direction information whether the illuminance is strengthened or weakened. If only the variance is applied, the light sensor will face the same drawback as the magnetic sensor.

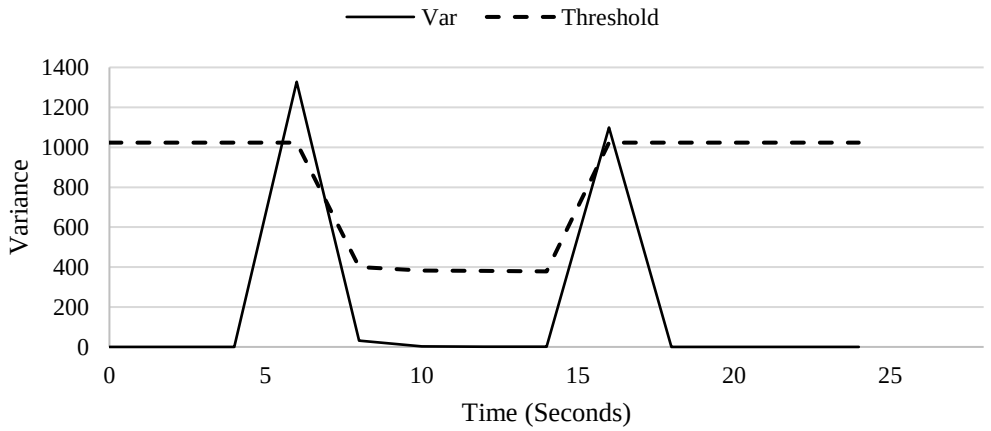

(a) Variance at Daytime

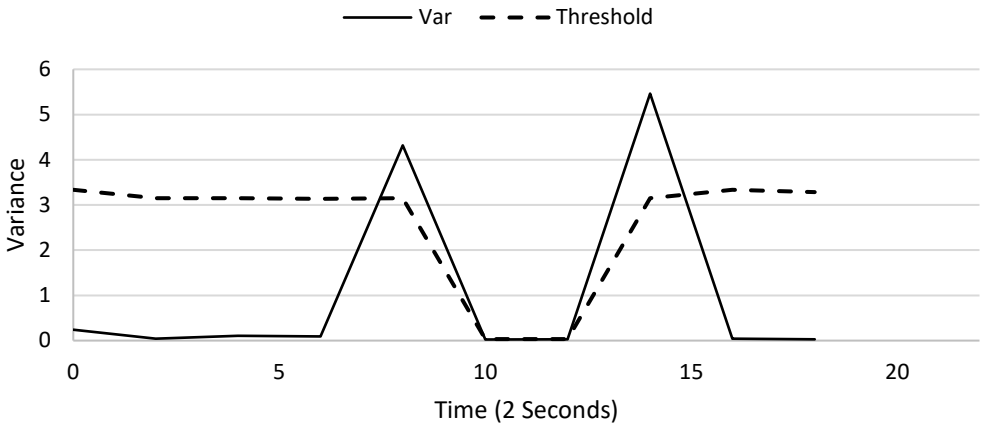

(b) Variance at Night

Figure 4.11 Variance Change when Occupancy Status Changes

4.2.3 *Change Rate Computation*

However, the illuminance change is directly correlated to the occupancy status change. When the SRS is occupied by a vehicle, the illuminance will definitely decrease. Therefore, the change rate is important for the light sensor. The expression of change rate is shown in Equation (4-11). And $T_2, T_3 > 0$ are thresholds to distinguish whether the change rate is great enough for a status change. The T_2 is the positive threshold and T_3 is the negative threshold. Firstly, the positive and negative of this rate will show the change direction. There are three possible scenarios for R_1, which are list below.

1) When $R_1 > T_2$, it indicates the illuminance change positively and the occupancy status of the SRS becomes empty.
2) When $R_1 < T_3$, it indicates the illuminance change negatively and the occupancy status of the SRS becomes occupied.

3) When $T_3 \leq R_1 \leq T_2$, it indicates there is no significant illuminance change. This scenario happens when a vehicle passes over the SRS without a stop. Although there is a sudden illuminance change, but this change is temporarily and does not last for a relatively long time. This scenario should be filtered as a result.

$$R_1 = \frac{D[n] + D[n-1] - (D[1] + D[2])}{max(D[n] + D[n-1], D[1] + D[2])} \quad (4\text{-}11)$$

4.3 Ultrasonic Sensor Detection Algorithm

The ultrasonic sensor is an important and effective sensor to detect the occupancy by measuring the distance between the top of SRS and a vehicle bottom which is similar to the vehicle ground clearance. Similar to the light sensor, the occupancy change will lead to a certain distance change. But the distance change scale has a specific boundary, which is better than the light sensor. In the open parking area, the maximum distance is equal to the maximum detection distance. And the minimum distance is equal to the vehicle ground clearance with ignoring the height of the SRS.

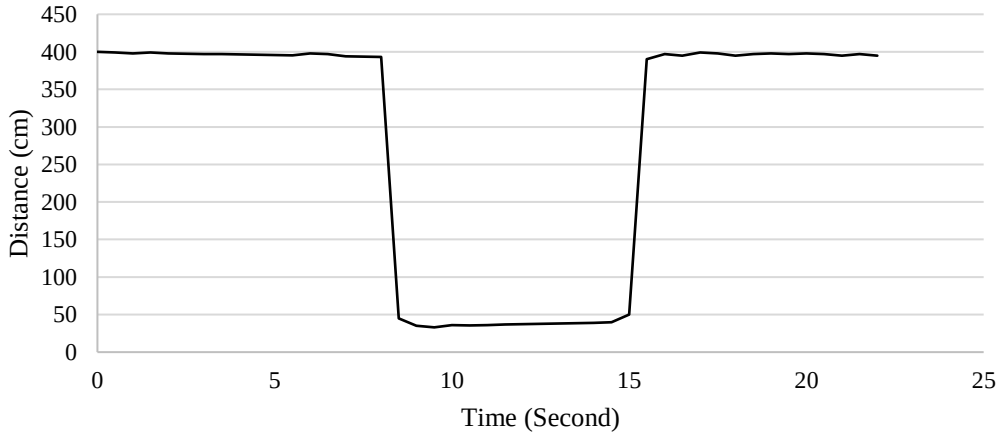

Figure 4.12 Ultrasonic Sensor Output

The ultrasonic sensor output is shown in Figure 4.12 which was collected in an open parking area. When there is no vehicle over the SRS, the output distance is $400cm$. When the vehicle is over the SRS, the distance decreases to the ground clearance height which is about $30cm$.

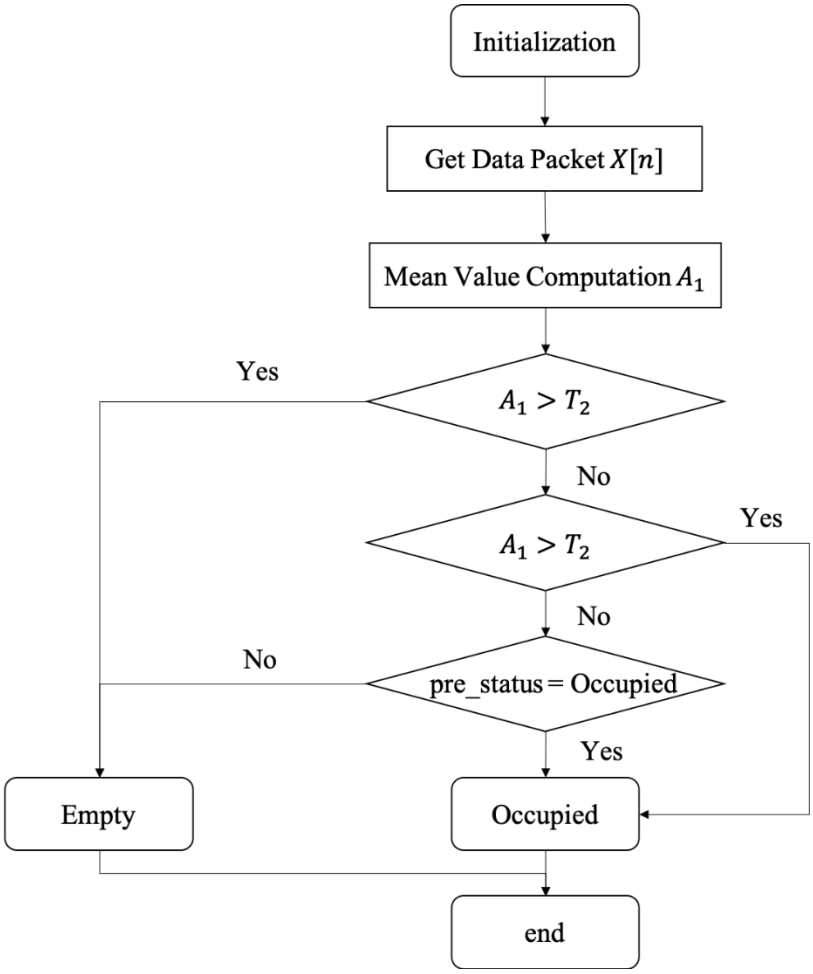

Figure 4.13 Ultrasonic Sensor Detection Algorithm

The ultrasonic sensor has a very direct output comparing with magnetic sensor and light sensor, which simplify its detection algorithm by reducing the wavelet transform and variance computation. The ultrasonic sensor detection algorithm is shown in Figure 4.13. The first step is collecting N sample points and computing their mean value A_1. The expression is shown in Equation (4-12). After that, A_1 will be compared with two thresholds T_1 and T_2, which are defined

as lower and upper boundaries respectively. There are three different relationships between A_1 and T, which are listed below.

1) When $A_1 < T_1$, it indicates that the detection distance is lower than the lower boundary. This happens when something falls on the sensor surface and blocks the ultrasonic waves. In this scenario, the ultrasonic sensor is disabled and cannot detect the occupancy. It thus will return the previous status.
2) When $A_1 > T_2$, it indicates there is no vehicle over the SRS and the occupancy status becomes empty.
3) When $T_2 \leq A_1 \leq T_1$, it indicates there is a vehicle in the detection range defined before, and the occupancy status becomes occupied.

$$A_1 = \frac{1}{N}\sum_{n=1}^{N} X[n] \tag{4-11}$$

4.4 SENSOR FUSION ALGORITHM

The sensor fusion algorithms have two versions based on different sensor sets. The first version is suitable for the SRS Version One with magnetic sensor and light sensor. And the second version is suitable for the SRS Version Two with magnetic sensor and ultrasonic sensor. The evaluation index of these algorithms is the detection accuracy or detection error rate. Based on the causes of the detection error, they can be divided into two categories – type I and type II errors, whose

concepts are drawn from the statistical hypothesis testing. And the four error types are shown in Table 4.2.

Table 4.2 Error Types of SRS Detection Algorithm

Error Types		Status Change in Practice	
		True	False
Status Change in SRS	Fail to Detect	Type II Error False Negative	True Positive
	Detect	True Negative	Type I Error False Positive

The type I error is defined as the rejection of a true null hypothesis, which is also called “false positive”. In this paper, the type I error is described as detecting the change when there is no status change in practice. Take the SRS with the single magnetic sensor as an example. The SRS may detect the parking status change when a heavy vehicle passes by and generates a great magnetic field distortion. The type I error can be reduced by using a secondary sensor to verify the detection results of magnetic sensor. If both sensors detect a status change, then the SRS will output current status via LoRa to nearby base station.

The type II error is defined as the failure to reject a false null hypothesis, which is also called “false negative”. In this paper, the type II error is defined as failing to detect the change when there is a status change in practice. Still take the SRS with the single magnetic sensor as an example. The SRS may fail to detect the status change when the magnetic distortion generated by the vehicle does not reach the threshold. This happens when the vehicle does not contain much ferromagnetic material. The type II error can be reduced by two possible ways. The first way is using the ultrasonic sensor as the secondary sensor to measure the distance with a longer interval. If the ultrasonic sensor finds a big distance change, then the SRS will send the current status. The second

way is using the light sensor to detect illuminance change using the algorithm shown in Figure 4.12. If the magnetic sensor does not detect the status change, the light sensor detects a status change and the minimum illuminance is higher than a threshold. The SRS will then send the current status. As a result, the sensor fusion algorithms applied in the SRS Version One is shown in Figure 4.14 and the algorithm applied in the SRS Version Two is shown in Figure 4.15.

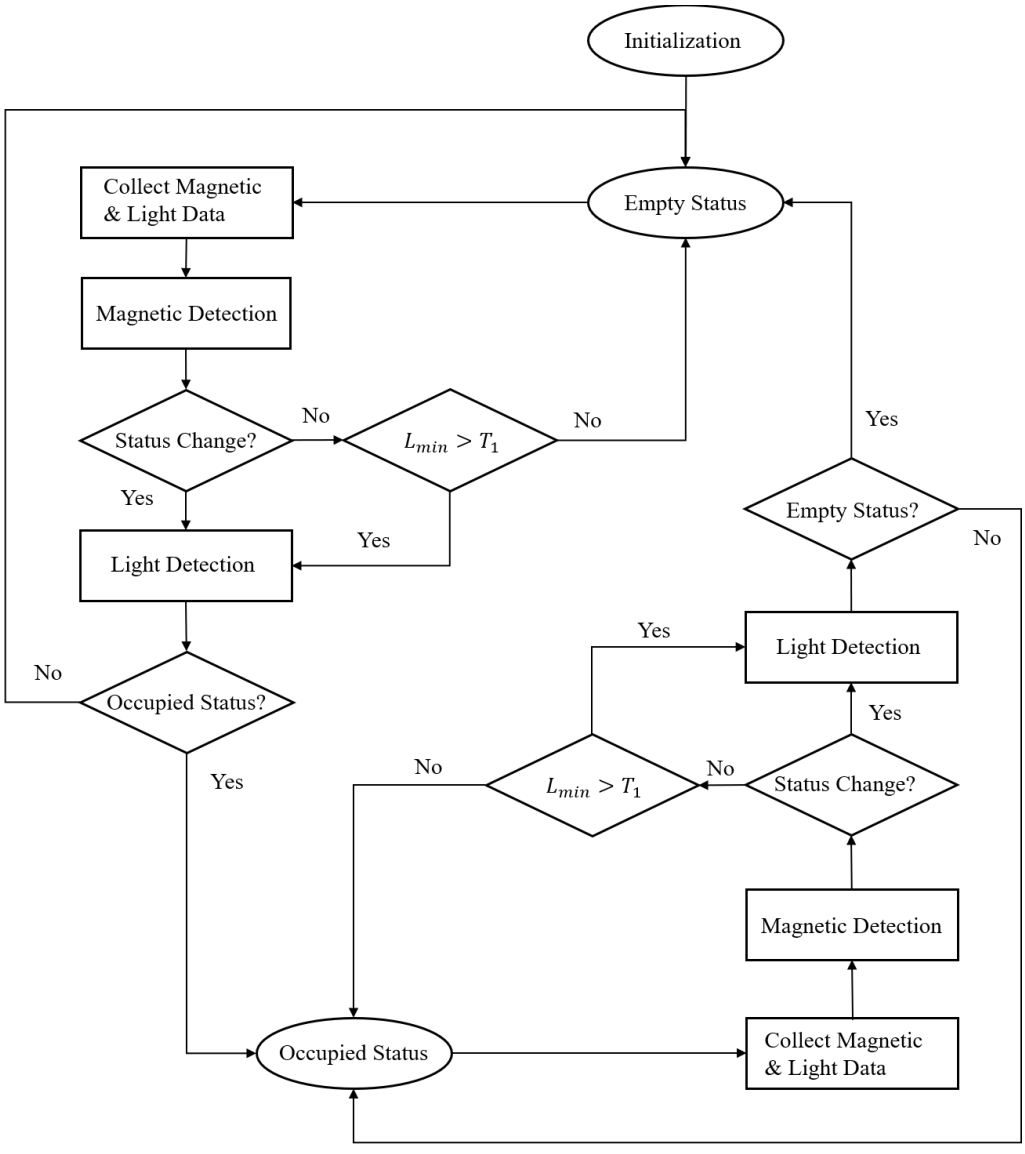

Figure 4.14 Sensor Fusion Algorithm of SRS Version One

According to Figure 4.14, the magnetic sensor performs as the primary sensor and the light sensor. When the magnetic sensor detects the status change, the light sensor will verify its detection results and will also detect the change direction. If the magnetic sensor does not detect the status change, it may indicate that the magnetic field distortion is weak. In order to further explore whether there is a status change, the light sensor will firstly measure the minimum illuminance L_{min} in the previous magnetic sensor detection period. The computation expression is shown in Equation (4-12) where the $X[i]$ is the illuminance at each sample point. If the minimum illuminance is higher than the threshold T_1, the light sensor will be triggered for detection. If the minimum illuminance is lower than the threshold, the illuminance is considered to be too weak for detection.

$$L_{min} = \min_i X[i] \tag{4-11}$$

Compared with the detection algorithm in SRS Version One, the detection algorithm in the SRS Version Two is more straight forward because the ultrasonic sensor can measure the distance between the SRS and vehicle bottom. This distance change has significant value change and directionality. If the vehicle occupies this space, the distance will decrease and vice versa. When the magnetic sensor detects the status change, the ultrasonic sensor will measure the distance and verify the detection results. If the magnetic sensor does not detect the status change for a "long time", the ultrasonic sensor will be triggered for detection. The time interval for triggering the ultrasonic sensor T_{inter} is defined as the time interval from last status change time to present time. And T_1 is the threshold of "long time".

These two detection algorithms have similar framework and take the magnetic sensor as the primary sensor. And the light or ultrasonic sensor plays as the secondary sensor to verify the

detection results of primary sensor and to make up the missing detection as well. And their performances are shown in the Chapter 5 by two field tests.

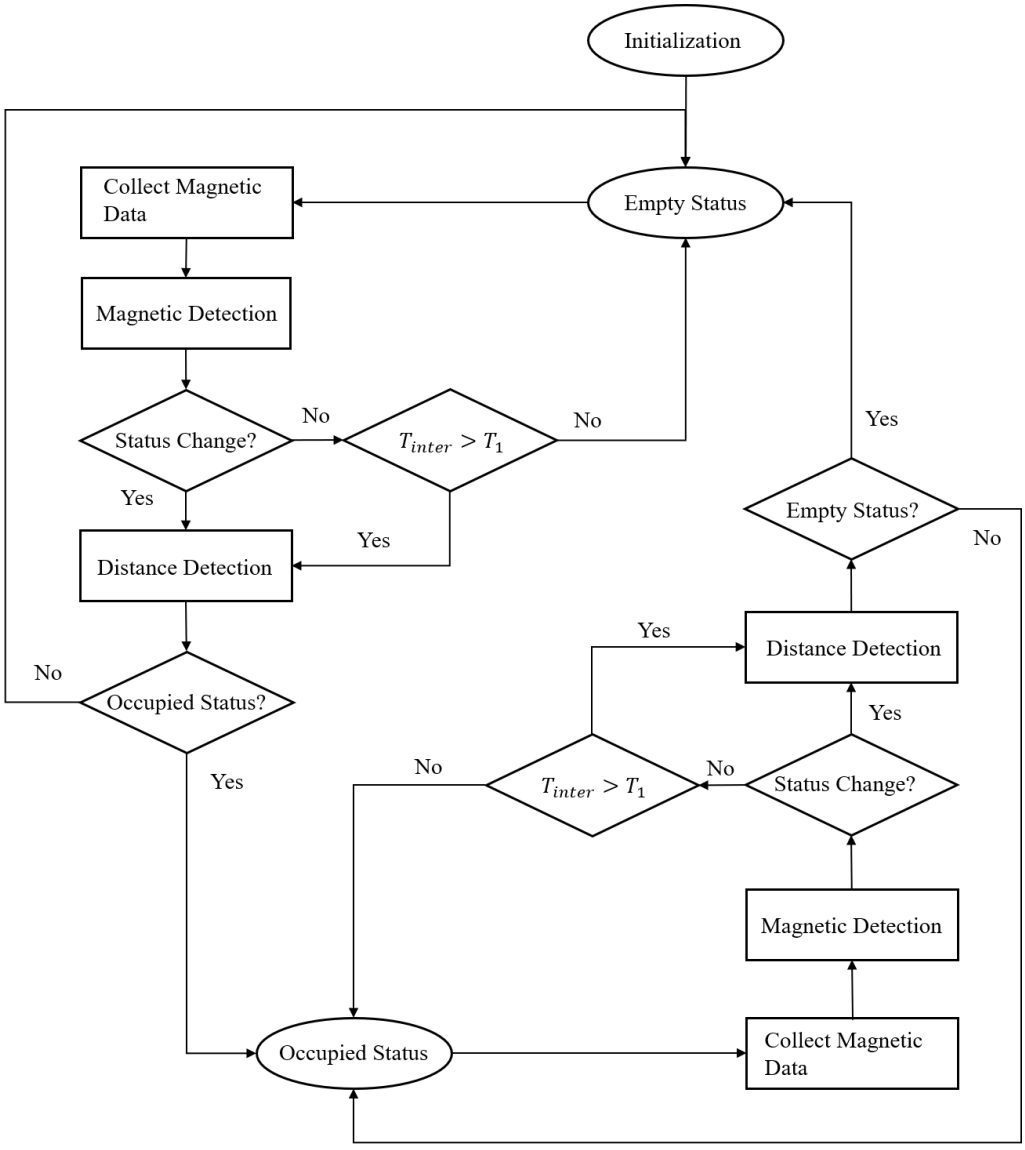

Figure 4.15 Fusion Algorithm of SRS Version Two

Chapter 5. FIELD TESTS

After making the hardware of SRS and developing the software, one power consumption test and two field tests were done to test different versions of SRSs and detection algorithms. There were four versions of SRS to be tested. The difference lies in the sensor combination and is shown in Table 5.1. The power consumption test was taken in laboratory setting on two kinds of SRS. One field test was taken in Angle Lake Parking Garage, while another field test was later taken in E18 Parking Lot at the University of Washington.

Table 5.1 SRS Version and Sensor Combination

SRS Version	Sensor Combination
SRS Version One	Magnetic + Light
SRS Version Two	Magnetic + Ultrasonic
SRS Type A	Magnetic
SRS Type B	Light

5.1 POWER CONSUMPTION TEST

Before testing the detection accuracy of SRS, the power consumption, which is another important specification of SRS, was tested in the laboratory firstly. Considering its installation locations and amount, it is hard to provide the external power supply or to replace the battery regularly, which requires that the SRS must have a long durability. The evaluation index of the power consumption is the average current. Although the evaluation index of battery life is clearer and more direct than the average current, the battery life does not only depend on the average current but also the battery volume. If the battery life is considered as the evaluation index, one more variable of battery volume should be added. Using battery life makes it difficult to compare power efficiency with

different battery volumes.

The average current varies based on the detection frequency and the transmission frequency. Higher sample rate indicates higher resolution which produces better detection results. However, higher sample rate will also lead to higher average current by increasing the time at active mode. It is a trade-off between the detection frequency and average current. Through comparing the power consumption of three modules – sensor module, CPU and communication module, it can be observed that the communication module consumes the most power when transmitting data. Therefore, the average currently also highly depends on the total transmission time. When the occupancy status changes frequently, the power consumption will be high since it is always in transmission mode to send data to nearby base station. When the occupancy status changes rarely, the SRS will be in standby mode for most time. Different detection and transmission frequencies are tested in this section to simulate different application scenarios from frequent status changes to rare status change.

The power consumption results of SRS Version One with different detection and transmission frequencies are shown in Table 5.2. The battery life is chosen as the evaluation index which can provide an intuitive feeling, and it is all computed based on the $6{,}000mAh$ LiPo battery. To clarify this part more clearly, three variables are defined -- f_{dp}, f_{ds} and T_s. The f_{dp} is the detection frequency of the primary sensor which is the magnetic sensor in this paper, and the f_{ds} is the detection frequency of the secondary or assisting sensor which is the light sensor or ultrasonic sensor in this paper. The detection frequency reflects the sensor operation rate which is not related to the occupancy status change. The unit of detection frequencies f_{dp} and f_{ds} are both Hz. T_s is the wireless transmission period and its unit is second(s). T_s reflects the occupancy status change frequency. The shorter T_s indicates that the status changes more frequently. There are six scenarios

to test for the power consumption of SRS Version One.

Table 5.2 Power Consumption of SRS Version One

	Average Current	Battery Life
Mode A	$8.80mA$	28 days
Mode B	$1.36mA$	184 days
Mode C	$0.74mA$	338 days
Mode D	$0.55mA$	455 days
Mode E	$1.23mA$	203 days
Mode F	$0.10mA$	$>$ 3 years

1) Mode A: This is the most active mode when $f_{dp} = 20Hz$, $f_{ds} = 20Hz$ and $T_s = 2s$. In this mode, all components including sensor module, CPU and communication module will keep active permanently. In the rest of the following modes, components will go to sleep or standby mode when not working.
2) Mode B: This mode has the same parameters as Mode A. But the difference lies in that all components will go to sleep or standby mode when they do not have calculation, detection or transmission work. The parameters are $f_{dp} = 20Hz$, $f_{ds} = 20Hz$ and $T_s = 2s$.
3) Mode C: This mode simulates the application scenario when the occupancy status changes every 5 minutes and the sensors are in the most active mode. The parameters are $f_{dp} = 20Hz$, $f_{ds} = 20Hz$ and $T_s = 300s$.
4) Mode D: This mode simulates the same scenario as the Mode B. But the detection frequency reduces to half of Mode B. The parameters are $f_{dp} = 10Hz$, $f_{ds} = 10Hz$ and $T_s = 300s$.
5) Mode E: This mode simulates the same scenario as the Mode A, But the detection frequency reduces to half of Mode A. The parameters are $f_{dp} = 10Hz$, $f_{ds} = 10Hz$ and $T_s = 2s$.
6) Mode F: This is the deep sleep mode without detection operation. In this mode, the SRS only

sends its status every 5 minutes and does not initiate detection function. The parameters are $f_{dp} = 0Hz$, $f_{ds} = 0Hz$ and $T_s = 300s$.

And the power consumption results of SRS Version Two are shown in Table 5.3. There are six scenarios to test for the power consumption of SRS Version Two. Different from previous modes for the SRS Version One, the detection frequency of secondary sensor is lower since the ultrasonic sensor does not require multiple sample points to determine the distance.

Table 5.3 Power Consumption of SRS Version Two

	Average Current	Battery Life
Mode A	$12.3mA$	20 days
Mode B	$3.01mA$	83 days
Mode C	$0.92mA$	272 days
Mode D	$0.72mA$	347 days
Mode E	$2.82mA$	89 days
Mode F	$0.20mA$	$>$ 3 years

1) Mode A: This is the most active mode when $f_{dp} = 20Hz$, $f_{ds} = 1Hz$ and $T_s = 2s$. In this mode, all components including sensor module, CPU and communication module will keep active permanently. In the rest of the following modes, components will go to sleep or standby mode when not working.
2) Mode B: This mode has the same parameters as Mode A. But the difference lies in that all components will go to sleep or standby mode when they do not have calculation, detection or transmission work. The parameters are $f_{dp} = 20Hz$, $f_{ds} = 1Hz$ and $T_s = 2s$.
3) Mode C: This mode simulates the application scenario when the occupancy status changes every 5 minutes and the sensors are in the most active mode. The parameters are $f_{dp} = 20Hz$,

$f_{ds} = 1Hz$ and $T_s = 300s$.

4) Mode D: This mode simulates the same scenario as the Mode B. But the detection frequency reduces to half of Mode B. The parameters are $f_{dp} = 10Hz$, $f_{ds} = 0.5Hz$ and $T_s = 300s$.
5) Mode E: This mode simulates the same scenario as the Mode A, But the detection frequency reduces to half of Mode A. The parameters are $f_{dp} = 10Hz$, $f_{ds} = 0.5Hz$ and $T_s = 2s$.
6) Mode F: This is the deep sleep mode without detection operation. In this mode, the SRS only sends its status every 5 minutes and does not initiate detection function. The parameters are $f_{dp} = 0Hz$, $f_{ds} = 0Hz$ and $T_s = 300s$.

5.2 Angle Lake Parking Garage Field Test

One test site was in the Angle Lake Parking Garage, which has more than 1,000 parking spaces. This garage is operated by Sound Transit. This parking garage is always very busy during the daytime from 7:00 am to 8:00 pm, because it is designed for transit parking and free to the public with the limit of single -time parking time up to 24 hours. Usually, travelers park their vehicles in this garage and then take trains to their destinations. It is important for Sound Transit managers to learn the parking patterns in this garage. Therefore, they can optimize the parking rules and provide more parking availability information to travelers who currently spend a lot of time finding an empty parking space. This test was taken from September to December in 2018 for about three months. Totally two types of SRS were tested in this parking site. The first type called SRS Type A used a single magnetic sensor for vehicle detection. The only difference between SRS Type A and SRS Version One is that the SRS Type A does not integrate light sensor with magnetic sensor. The second type called SRS Version Two used both magnetic and ultrasonic sensor.

There were three locations in this garage adopted for this test, which were 15-minute parking, HOV-permit parking and regular parking. The 15-minute parking area, which was chosen on the ground floor, provided a pick-up place for travelers since the vehicles do not need to enter the garage. The HOV-permit parking area, which was chosen on the third floor, was only open to vehicles with HOV-permit from 4:00 am to 8:30 am. Regular parking area, which was chosen on the sixth floor, was open to all vehicles with "first come first served" policy. Considering that Angle Lake Parking Garage was just one stop away from the airport and was free, it became important to avoid travelers parking here for flight, which violated the original design intention. Therefore, the maximum parking time for all parking areas except 15-minute parking area were set as 24 hours. These three kinds of locations were the most representative scenarios for a parking garage.

However, there was no effective detection tool or method for the Angle Lake Parking Garage to learn the parking pattern or to detect the parking violation. Before this test, all work was done manually. It was hard to get the real-time parking occupancy information without state-of-the-art methods. Therefore, the SRS system was a proper option for this parking site to provide real-time occupancy information with limited installation workload.

5.2.1 *Installation Process*

There are 18 SRS installed in this parking site. Considering that the magnetic sensor in SRS is sensitive to axles of the vehicle, the desired position for SRS installation should be near the center of each parking slot. Thus, the front or rear axle can go over the SRS. The installation position is shown in Figure 5.1. Figure 5.1 (a) is the schematic installation position with exact distance. The distance between the installation position and the front of the parking slot is $2{,}000mm$. And it is

also at the center on the x-axis and its distance to the origin point is $1{,}250mm$. Figure 5.1 (b) shows the practical installation position, where the dash circles mark those installation positions of SRS.

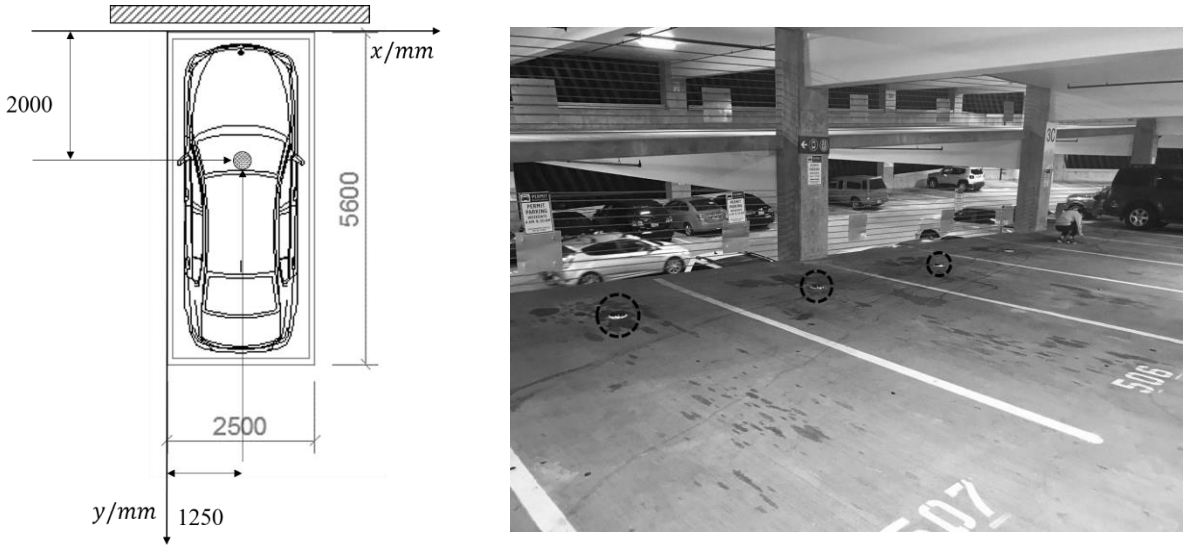

(a) Schematic Installation Position (b) Practical Installation Position

Figure 5.1 Installation Position of SRS

(a) Installation Process (b) SRS after Installation

Figure 5.2 Installation Process of SRS

The installation process is shown in Figure 5.2. Figure 5.2 (a) shows the process of mounting the SRS on the parking slot surface using epoxy resin adhesive. The installation is convenient since only adhesive is required without any driller. Figure 5.2 shows the SRS after installation. In order

not to influence the efficiency of the solar panel on the top of SRS, adhesive should be avoided on the surface of the solar panel. And the installation steps are shown in Table 5.4 below.

Table 5.4 SRS Installation Process

1) Close the parking slot before the installation and clean the ground surface.
2) Apply epoxy resin adhesive on the ground surface and bottom of the SRS.
3) Place the SRS on the ground and use heavy item weighing about $3kg$ on top of SRS to make it tight to the ground.
4) Wait about 2 hours for adhesive curing.
5) Open the parking slot with the SRS installed.

5.2.2 *Test Results*

After 3-month testing in the Angle Lake Parking Garage, both the SRS detection results and the ground-truth data were collected using the surveillance video camera. The parking status in the video was marked manually as the comparison with the parking status from SRS. The detection accuracy was then computed by comparing the detection results and ground truth data. The overall detection accuracy of the SRS is shown in Table 5.5.

The average detection accuracy of SRS Type A is 85.6%. The SRS Type A was installed on the third and sixth floor, and its detection accuracy is different on different floors. It is higher on the sixth floor than the third floor since the concrete building structure has more impacts on the third floor. What's more, it is also higher on the weekend than the weekend since there were fewer passing-by vehicles which might cause disturbance on the magnetic field and then influence detection results. The SRS Version Two was installed on the third floor and ground floor. And the

average detection accuracy is more than 99.9%, which proves the importance of sensor fusion and effectiveness of the ultrasonic sensor.

Table 5.5 Detection Accuracy of SRS

	SRS Type A	SRS Version Two
Average	85.6%	>99.9%
Ground Floor (Weekday)	N.A.	>99.9%
Ground Floor (Weekday)	N.A.	>99.9%
Third Floor (Weekday)	81.7%	>99.9%
Third Floor (Weekend)	89.3%	>99.9%
Sixth Floor (Weekday)	88.9%	N.A.
Sixth Floor (Weekend)	93.0%	N.A.

As well as the detection accuracy, the parking patterns were also analyzed, which was another important task for this test. The parking occupancy in the regular parking area is shown in Figure 5.3. There were totally 10 parking slots installed with SRS on the sixth floor. The average parking time in weekdays were around 10.5 hours while it became 3.9 hours in weekends. According to Figure 5.3, the parking slots were occupied between 7:00 am to 7:30 am in weekdays. And they were gradually empty after 4:00 pm and would be cleared after 6:00 pm. And On weekends, the parking slots were not fully occupied since there were empty parking slots on lower levels such as third floor. Drivers would park their vehicles near the entrance.

The parking occupancy in the HOV-permit parking area is shown in Figure 5.4. There were totally 6 parking slots installing SRS on the third floor. The average parking time in weekdays was around 10.4 hours while it became 6.5 hours on weekends. When comparing with occupancy distribution in regular parking area, the full occupied time was later because only vehicles with permit could park in this area before 8:30 am. Drivers with this permit did not need to come early

to take a position. One interesting phenomenon was that these slots were also cleared later since some vehicles might come in the afternoon and park there until midnight. On the weekend, the occupancy of these parking slots was obviously higher than regular parking area on the sixth floor because they were closer to the garage entrance and there was also no permit limitation.

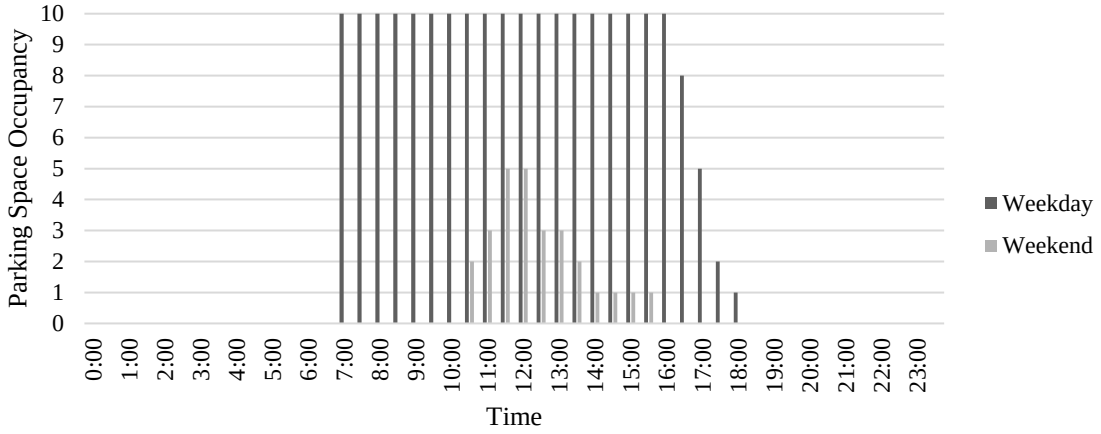

Figure 5.3 Parking Occupancy in Regular Parking Area

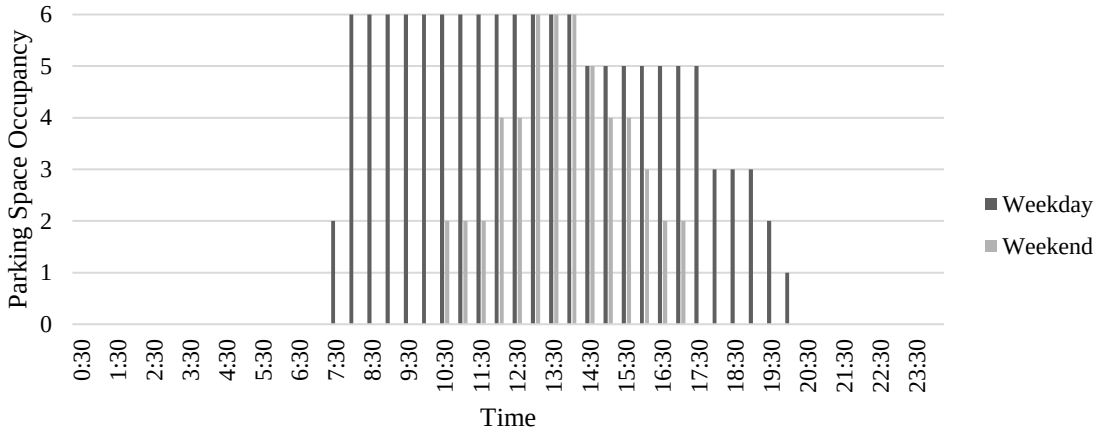

Figure 5.4 Parking Occupancy in HOV-permit Parking Area

Considering the average parking time in 15-minute parking area is relatively short and only two SRS were installed in this area, the parking occupancy is not used here. Otherwise, the parking duration and frequency are used for analysis, which are shown in Figure 5.5. According to Figure

5.5 (a), the parking peaks happened between 3:00 pm to 5:00 pm when travelers got back from work on weekday. One phenomenon was that there were fewer vehicles in the morning when travelers went to their workplace. Figure 5.5 (b) shows the parking duration distribution, where each column shows the average parking duration in that time interval. The parking duration on weekend was generally higher than the weekday since this parking area was not as busy as usual. The maximum parking duration detected was 152 minutes. Therefore, the SRS system is important to monitor the parking status in 15-minute parking area and to reduce the violation frequencies.

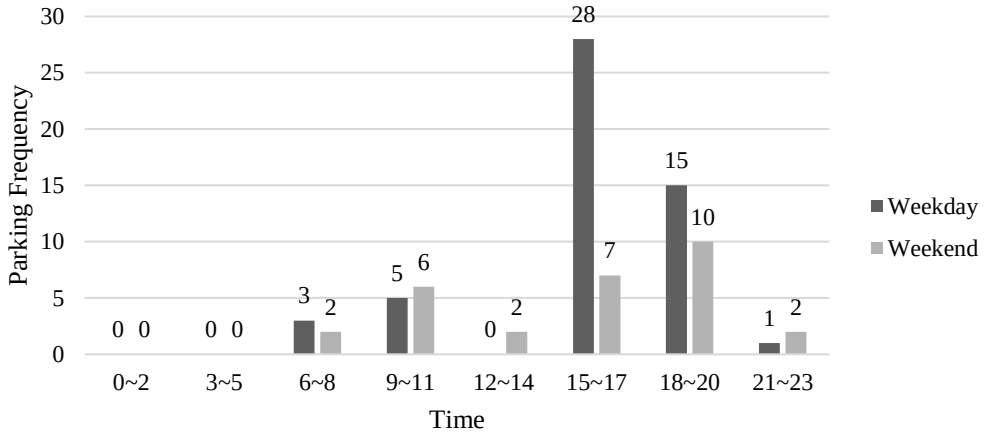

(a) Parking Frequency

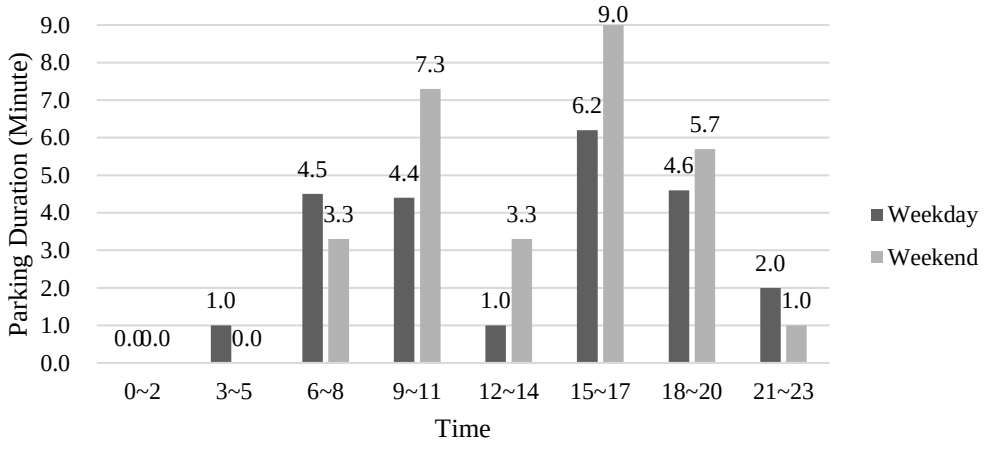

(b) Parking Duration

Figure 5.5 Parking Patterns in 15-minute Parking Area

5.2.3 *Existing Problems*

According to the test results, the detection accuracy of the SRS Type A with the single magnetic sensor was much lower than previous research work or practical products are done by others which were all more than 90% or even 95%. After analyzing the test results, there are several problems to be addressed.

The first problem is the uncertain parking status which could not be decided by the magnetic sensor independently. The core of this problem is that the magnetic sensor can only detect the status change. The magnetic field change when a vehicle enters or leaves a parking slot does not have much difference. It is hard to distinguish the change direction based on the magnetic field change. The change direction varies according to different external conditions such as vehicle types and installation positions. This problem stands out especially for the SRS with single magnetic sensor for the parking application. If one status change was missed, the status recorded by the SRS after that would be all opposite to the real status. This phenomenon was not addressed before because most application scenarios were counting vehicles rather than detecting parking status. In the application of counting, one status change was considered as one vehicle. Even if one vehicle was missed, it would not influence the later results. However, this problem could not be solved only by algorithms based on above reasons. One solution to this problem is using the sensor fusion method by adding one or more sensors, such as ultrasonic sensor and light sensor, to assist the magnetic sensor. The assisting sensors share one feature that they can detect the current occupancy status independently. The reason for not replacing the magnetic sensor lies in that it is suitable for most applications while other sensors have more limitations as the major sensor.

The second problem was the weak waterproof of the SRS. Although the test site was an indoor parking garage, there was still a lot of water vapor getting into the SRS and erode the PCB and

battery without strong water resistant. The waterproof was considered but underestimated before the installation by sealing all junction parts. This work was far more enough to prevent water vapor. The first batch of six SRS did not survive for more than two days after the installation. Most SRS died on the second morning when the water vapor was the most serious at that time. Through disassembling all these SRS, both PCB and battery was eroded totally and could not get back to work anymore. The current on the PCB even accelerated the erosion process. The solution to this problem was filling the inside of SRS with electronic epoxy resin to prevent all electronic components from the water. When filling the inside of the SRS Version Two, it should be careful not to let the side of the ultrasonic probe get in touch with the epoxy resin which would influence the detection performance. After adopting this method, the battery life extended significantly.

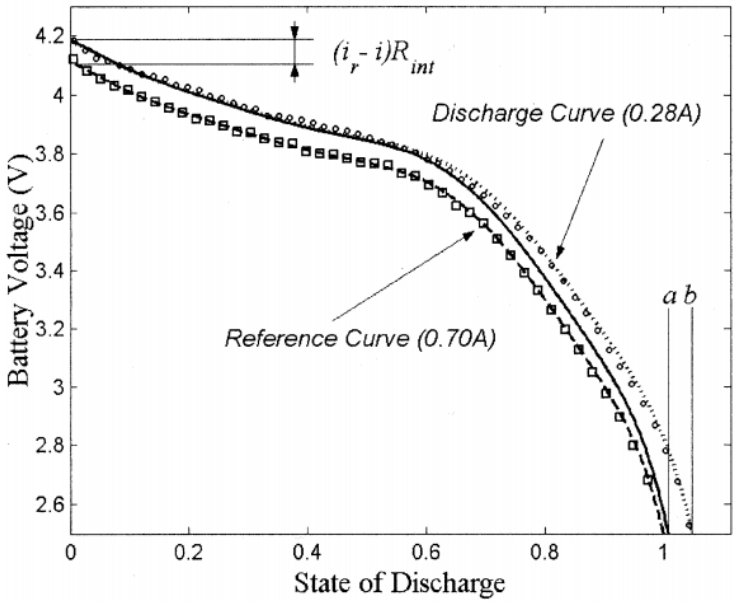

Figure 5.6 Discharge Curve of LiPo Battery [79]

The third problem was the power efficiency and service life of SRS. During this test, it was found that the battery life was shorter than the expectation. The main reason was the battery. Though the battery volume was 6,000mAh, it could not be fully used according to the discharge

curve shown in Figure 5.6. When the volume dropped below one threshold, it could not output any power. In addition, higher operating current would make the curve steeper which indicated that the threshold would be higher [79]. The available volume can be used was around 80% of the total volume indicated on the battery. Another reason was that the components still consume too much power. This could be improved by replacing with new power-efficient chips to save more power.

Although the detection accuracy of the second type reached 100%, there were two problems found in this test. The first problem of assembling the ultrasonic sensor would influence the mass production in the future. Due to the detection principle of the ultrasonic sensor, the side of ultrasonic probe could be touched by solid material such as SRS case. Once it was touched, the output of the ultrasonic sensor would be greatly influenced and could not measure the distance. Therefore, the assembling process should be careful to avoid the probe getting in touch with the top case. And this feature led to the quality control becoming hard. One solution to this problem was applying an ultrasonic sensor with the support which was touchable and waterproof. Another was the blocking of the ultrasonic sensor by leaves or other items. When blocked by other things, the ultrasonic sensor could not work properly. And these things could only be removed manually. The solution was that the SRS would send cleaning message when the output distance of the ultrasonic sensor was lower than one threshold for a relatively long time.

5.3 E18 PARKING LOT FIELD TEST

The second testing site was an open parking area in the University of Washington. Three types of SRS were tested on this site. The first type was the SRS Type A with improved detection algorithm and the second type was called the SRS Type B which only applied the single light sensor. The third type was the SRS Version One. After learning from the first test in Angle Lake Parking

Garage, a lot of improvement work has been done to increase the detection accuracy and the robust of the SRS.

5.3.1 *Test Results*

The testing results indicated that there was a great progress on the detection accuracy aspect. Both types of SRS achieved more than 95% detection accuracy in different scenarios. In order to simulate the practical parking situation of a vehicle passing over the SRS without stopping, the passing-by was added at two different speeds. The high passing-by speed was over $8mph$ and the low passing-by speed was below $8mph$. The speed threshold was computed by the magnetic sensor detection frequency and the average vehicle length. The test result of SRS Type A is shown in Table 5.6.

Table 5.6 Detection Accuracy Using SRS Type A

Detection Event	Accuracy
Detecting all vehicles (including passing-by vehicles)	$91.2\%\ (73/80)$
Detecting parking vehicles	$95.7\%\ (67/70)$
Detecting passing-by vehicles (Speed $\leq 8mph$)	$100\%\ (5/5)$
Detecting passing-by vehicles (Speed $> 8mph$)	$0\%\ (0/5)$

The detection accuracy improved significantly when compared with the test results in the Angle Lake Parking Garage from 86% to 91%. From Table 5.3, it can be observed that all detection results were wrong when a vehicle passed over the SRS at a "high" speed of $8mph$. Limited to the detection algorithm of using a window for analysis, two status changes were too close and combined into one. Thus, the SRS Type A could only detect one status change rather than two

changes. For example, if the initial status is empty, it would change from empty status to occupied status and not go back to empty status.

In order to overcome this problem, the light sensor was added as the assisting sensor. Before applying the sensor fusion, the light sensor was tested individually. Considering the light sensor is sensitive to the environmental light, thus the test was done at day time and night. The basic illuminance at day time was $12{,}000Lux$, and it was $50Lux$ at night. The test result at day time is shown in Table 5.7 and the result at night at night is shown in Table 5.8. It can be observed that the detection accuracy of SRS Type B at night was lower than the day time because the illuminance change scale was smaller when the external light became darker. But the detection accuracy at night was still in a reasonable range and was higher than 85%.

Table 5.7 Detection Accuracy Using SRS Type B (Day Time)

Detection Event	Accuracy
Detecting all vehicles (including passing-by vehicles)	$96.3\%\ (77/80)$
Detecting parking vehicles	$97.1\%\ (68/70)$
Detecting passing-by vehicles (Speed $\leq 8mph$)	$80.0\%\ (4/5)$
Detecting passing-by vehicles (Speed $> 8mph$)	$100\%\ (5/5)$

Table 5.8 Detection Accuracy Using SRS Type B (Night)

Detection Event	Accuracy
Detecting all vehicles (including passing-by vehicles)	$87.5\%\ (70/80)$
Detecting parking vehicles	$92.9\%\ (65/70)$
Detecting passing-by vehicles (Speed $\leq 8mph$)	$40.0\%\ (2/5)$
Detecting passing-by vehicles (Speed $> 8mph$)	$60.0\%\ (3/5)$

After evaluating the effectiveness of the light sensor using the SRS Type B, the sensor fusion of combining magnetic sensor and light sensor was tested using the SRS Version One at both day

time and night. The test result at day time is shown in Table 5.9 and the result at night is shown in Table 5.10. Comparing the detection accuracy of sensor fusion algorithm with single magnetic sensor algorithm or light sensor algorithm, it can be found the average detection accuracy increased especially in the perspective of the passing-by vehicle at a fast speed. It also proved that the light sensor could help solve the problem of passing-by vehicles generating several peaks during one detection round of the magnetic sensor. What's more, the detection accuracy was higher when there was enough environmental light. The dark environment could be considered as a hinder of the light sensor. Although the light sensor did not perform well in the dark environment, it could still increase the overall accuracy.

Table 5.9 Detection Accuracy Using SRS Version One (Day Time)

Detection Event	Accuracy
Detecting all vehicles (including passing-by vehicles)	98.8% (79/80)
Detecting parking vehicles	98.6% (69/70)
Detecting passing-by vehicles (Speed $\leq 8mph$)	100% (5/5)
Detecting passing-by vehicles (Speed $> 8mph$)	100% (5/5)

Table 5.10 Detection Accuracy Using SRS Version One (Night)

Detection Event	Accuracy
Detecting all vehicles (including passing-by vehicles)	95.0% (76/80)
Detecting parking vehicles	97.1% (68/70)
Detecting passing-by vehicles (Speed $\leq 8mph$)	100% (5/5)
Detecting passing-by vehicles (Speed $> 8mph$)	60.0% (3/5)

5.3.2 *Existing Problems*

Although Problems showed up in the previous test were solved by improvement in both hardware and software, there were some new problems about the light sensor detection and the long-distance communication.

The first problem was that the light sensor did not perform well individually in the dim environment where the illuminance was even lower than $1Lux$. The illuminance change would be submerged in signal noise. The solution to this problem was ignoring detection results of light sensor when the minimum illuminance was too low. In the extremely dim environment, the SRS Version One only used the magnetic sensor for detection.

In addition, the vehicle light would also influence the light sensor in the dim environment. While in the bright condition, the illuminance of vehicle light would be comparable to or lower than the environment light. However, the vehicle light would be much brighter than environment light in the dim condition. If the light sensor was adherent to the top of the SRS, it was easily affected by the reflection light from other vehicles. The solution was lowering the light sensor, which is shown in Figure 5.7. The dash rectangular indicates the original position of the light sensor and the solid rectangular indicates the improved position. In this way, the light sensor could only receive the direct and reduce the reflected light to the utmost extent.

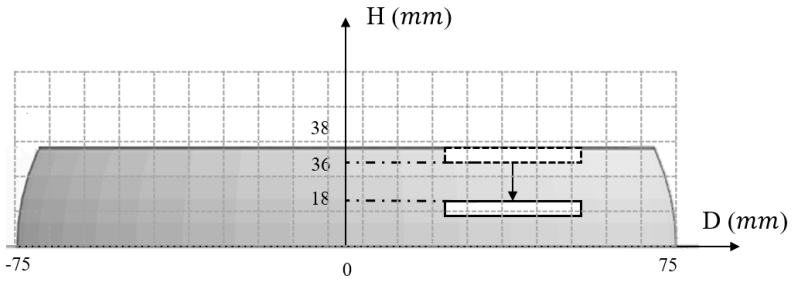

Figure 5.7 Light Sensor Placement

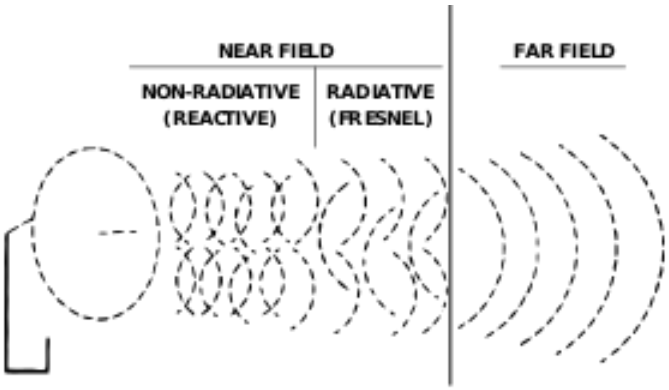

Figure 5.8 Antenna Operating Principle [80]

The second problem was shorter communication distance than the original expectation with a single wire antenna. The ideal communication distance is over $500m$, but the actual distance in test was less than $200m$. The reason lied in the placement of antenna. According to communication principle shown in Figure 5.8 [80], the basic idea is making full use of the radiative near field. Two typical placements are keeping the antenna vertical [81] or horizontal. The antenna bending will generate great influence on the communication performance. However, the antenna was bent randomly during the assembling process because of the limited inner space. As a result, the distance was shorter than the design. The solution without changing the case design was replacing the antenna with shorter overall length such as coil antenna [82]. With the same gain and operation frequency, the coil antenna has shorter length than the single wire length.

Chapter 6. CONCLUSIONS AND FUTURE PLAN

The fast city expansions primarily increase the number of vehicles. The increasing vehicle number then leads to higher demands for parking space. However, the existing parking facilities cannot meet this demand. The insufficiency of parking facilities has become more severe than ever, which does not only lead to traffic congestion but also wastes both traveler's time and society resources. Considering the shortage of land use in the urban area, it is difficult to expand parking space to a larger scale. Therefore, the improvement of parking management system by reducing the searching and waiting time is an effective solution to the current parking problem. The parking detection system is an important part of the management system. And its accuracy and robustness will significantly influence the ultimate performance of the whole system. Therefore, this paper focuses on upgrading the parking detection system by proposing an innovative wireless parking detector named SRS with sensor fusion and IoT communication technologies.

There are two types of SRS developed in this paper for different application scenarios, which are SRS Version One and SRS Version Two. The SRS Version One combines the magnetic and light sensor and is designed to deploy in the outdoor parking facilities. The SRS Version Two combines the magnetic and ultrasonic sensor and is targeted to be applied in the indoor parking facilities. The major contributions of this research work are making great improvements on parking detectors in both hardware and software perspectives. In the hardware perspective, a specific PCB is designed for parking detection. This PCB highly integrates sensor module, control module, communication module, and power module. The software perspective focuses on deeply improving existing detection algorithm based on magnetic sensor and ultrasonic sensor, and proposing new algorithms based on light sensor and sensor fusion.

Two field tests were carried out on different stages to evaluate the performance of the SRS. The first field test was done in the Angle Lake Parking Garage for more than three months. The detection accuracy of SRS Type A was more than 85%. And the SRS Version Two achieved detection accuracy of almost 100%. However, problems were also exposed, including insufficient accuracy and relatively short battery life. After this test, improvement work was done in the perspectives of improving the detection algorithms and replacing with power-efficient components. The second test was conducted at a parking lot on the campus of the University of Washington. The detection accuracy of SRS Type A increased from 86% to 91% with improved magnetic detection algorithm. And the detection accuracy of the SRS Version One was over 95%.

Based on current work, the future work will continue to further increase the detection accuracy and to enhance the system robustness in order to adapt to various environment. The first task will keep improving the fusion algorithm and increase the detection accuracy especially under the condition of dim light and complex magnetic field. The second task will optimize the sensor selection, like ultrasonic sensor. Currently, the ultrasonic sensor may be affected by the assembling process and the top SRS case. A new distance sensor will be adopted to avoid the influence of the case. The third task will extend its battery life by selecting more power-efficient components and reducing the time at active mode. Redundant components will be removed, and a new CPU will also be applied with lower operating current. The fourth task is building the standard for mass production including assembling guidance and quality control methods.

BIBLIOGRAPHY

[1] Markoff, John. "Can't find a parking spot? check smartphone." New York Times 12 (2008).

[2] B Kwon, Eil, and Sonia Pitt. "Evaluation of emergency evacuation strategies for downtown event traffic using a dynamic network model." Transportation Research Record: Journal of the Transportation Research Board 1922 (2005): 149-155.

[3] Arnott, Richard. "On the optimal target curbside parking occupancy rate." Economics of Transportation 3.2 (2014): 133-144.

[4] Downs, Anthony. Stuck in traffic: Coping with peak-hour traffic congestion. Brookings Institution Press, 2000.

[5] Knuth, Donald Ervin. The art of computer programming. Vol. 3. Pearson Education, 1997.

[6] Chinrungrueng, Jatuporn, Songphon Dumnin, and Ronachai Pongthornseri. "IParking: A parking management framework." 2011 11th International Conference on ITS Telecommunications. IEEE, 2011.

[7] Andersen, Johann, and Steve Sutcliffe. "Intelligent Transport Systems (ITS)-An Overview." IFAC Proceedings Volumes 33.18 (2000): 99-106.

[8] Cookson Graham, and Bob Pishue. Global Traffic Scorecard. Technical report, INRIX, 2017.

[9] Arnott, Richard, and Kenneth Small. "The economics of traffic congestion." American scientist 82.5 (1994): 446-455.

[10] Chin, Anthony TH. "Containing air pollution and traffic congestion: transport policy and the environment in Singapore." Atmospheric Environment 30.5 (1996): 787-801.

[11] Walters, Alan A. "The theory and measurement of private and social cost of highway congestion." Econometrica: Journal of the Econometric Society (1961): 676-699.

[12] Scellato, Salvatore, et al. "Traffic optimization in transport networks based on local routing." The European Physical Journal B 73.2 (2010): 303-308.

[13] Litman, Todd, and Steven B. Colman. "Generated traffic: Implications for transport planning." ITE journal 71.4 (2001): 38-46.

[14] Cheung Sing Yiu, et al. "Traffic measurement and vehicle classification with single magnetic sensor." Transportation Research Record 1917.1 (2005): 173-181.

[15] Park Sang Jin, et al. "A novel signal processing technique for vehicle detection radar." Microwave Symposium Digest, 2003 IEEE MTT-S International. Vol. 1. IEEE, 2003.

[16] Zhang Guohui, Ryan Avery, and Yinhai Wang. "Video-based vehicle detection and classification system for real-time traffic data collection using uncalibrated video cameras." Transportation Research Record: Journal of the Transportation Research Board 1993 (2007): 138-147.

[17] Heberley, Jeffrey R., et al. "Method for detecting extended range motion and counting moving objects using an acoustics microphone array." U.S. Patent No. 6,914,854. 5 Jul. 2005.

[18] Yang, Jihoon, Jorge Portilla, and Teresa Riesgo. "Smart parking service based on wireless sensor networks." IECON 2012-38th Annual Conference on IEEE Industrial Electronics Society. IEEE, 2012.

[19] Coleri, Sinem, Sing Yiu Cheung, and Pravin Varaiya. "Sensor networks for monitoring traffic." Allerton conference on communication, control and computing. 2004.

[20] Middleton, Dan R., Hassan A. Charara, and Ryan Longmire. Alternative vehicle detection technologies for traffic signal systems: technical report. No. FHWA/TX-09/0-5845-1. Texas Transportation Institute, Texas A & M University System, 2009.

[21] Oh, Cheol, Seri Park, and Stephen G. Ritchie. "A method for identifying rear-end collision risks using inductive loop detectors." Accident Analysis & Prevention 38.2 (2006): 295-301.

[22] Sun, Carlos, and Stephen G. Ritchie. "Individual vehicle speed estimation using single loop inductive waveforms." Journal of Transportation Engineering 125.6 (1999): 531-538.

[23] Gajda, Janusz, et al. "A vehicle classification based on inductive loop detectors." Instrumentation and Measurement Technology Conference, 2001. IMTC 2001. Proceedings of the 18th IEEE. Vol. 1. IEEE, 2001.

[24] Effects of Loop Detector Installation on the Portland Cement Concrete Pavement Lifespan: Case Study on I-5 (https://www.wsdot.wa.gov/research/reports/fullreports/744.5.pdf)

[25] Fang, Jianxin, et al. "A low-cost vehicle detection and classification system based on unmodulated continuous-wave radar." 2007 IEEE Intelligent Transportation Systems Conference. IEEE, 2007.

[26] Jeong, S. H., et al. "Low cost design of parallel parking assist system based on an ultrasonic sensor." International Journal of Automotive Technology 11.3 (2010): 409-416.

[27] Kianpisheh, Amin, et al. "Smart parking system (SPS) architecture using ultrasonic detector." International Journal of Software Engineering and Its Applications 6.3 (2012): 55-58.

[28] Park, Wan-Joo, et al. "Parking space detection using ultrasonic sensor in parking assistance system." 2008 IEEE intelligent vehicles symposium. IEEE, 2008.

[29] Liu, Xinchen, et al. "Large-scale vehicle re-identification in urban surveillance videos." 2016 IEEE International Conference on Multimedia and Expo (ICME). IEEE, 2016.

[30] Sun, Zehang, George Bebis, and Ronald Miller. "On-road vehicle detection using Gabor filters and support vector machines." 2002 14th International Conference on Digital Signal Processing Proceedings. DSP 2002 (Cat. No. 02TH8628). Vol. 2. IEEE, 2002.

[31] Bautista, Carlo Migel, et al. "Convolutional neural network for vehicle detection in low resolution traffic videos." 2016 IEEE Region 10 Symposium (TENSYMP). IEEE, 2016.

[32] Wu, Qi, et al. "Robust parking space detection considering inter-space correlation." 2007 IEEE International Conference on Multimedia and Expo. IEEE, 2007.

[33] Bulan, Orhan, et al. "Video-based real-time on-street parking occupancy detection system." Journal of Electronic Imaging 22.4 (2013): 041109.

[34] Ishida, Shigemi, et al. "Design of acoustic vehicle count system using DTW." Proc. ITS World Congress. AP-TP0678. 2016.

[35] Ding, Jiagen, et al. "Vehicle detection by sensor network nodes." (2004).

[36] Barbagli, Barbara, et al. "Acoustic sensor network for vehicle traffic monitoring." Proceedings of the 1st International Conference on Advances in Vehicular Systems, Technologies and Applications. 2012.

[37] Kumar, Rakesh, Naveen K. Chilamkurti, and Ben Soh. "A comparative study of different sensors for smart car park management." The 2007 International Conference on Intelligent Pervasive Computing (IPC 2007). IEEE, 2007.

[38] Shaikh, Faiz Ibrahim, et al. "Smart parking system based on embedded system and sensor network." International Journal of Computer Applications 140.12 (2016).

[39] Bachani, Mamta, Umair Mujtaba Qureshi, and Faisal Karim Shaikh. "Performance analysis of proximity and light sensors for smart parking." Procedia Computer Science 83 (2016): 385-392.

[40] Bugdol, Marcin, et al. "Vehicle detection system using magnetic sensors." Transport Problems 9 (2014).

[41] Wang, Qing, et al. "Roadside magnetic sensor system for vehicle detection in urban environments." IEEE Transactions on Intelligent Transportation Systems 19.5 (2018): 1365-1374.

[42] Markevicius, Vytautas, et al. "Dynamic vehicle detection via the use of magnetic field sensors." Sensors 16.1 (2016): 78.

[43] Guan, Xiangke, et al. "A vehicle detection algorithm based on wireless magnetic sensor networks." Communications and Networking in China (CHINACOM), 2013 8th International ICST Conference on. IEEE, 2013.

[44] Ding, Jiagen, et al. "Signal processing of sensor node data for vehicle detection." Intelligent Transportation Systems, 2004. Proceedings. The 7th International IEEE Conference on. IEEE, 2004.

[45] Bokareva, Tatiana, et al. "Wireless sensor networks for battlefield surveillance." Proceedings of the land warfare conference. 2006.

[46] Chellappa, Rama, Gang Qian, and Qinfen Zheng. "Vehicle detection and tracking using acoustic and video sensors." 2004 IEEE International Conference on Acoustics, Speech, and Signal Processing. Vol. 3. IEEE, 2004.

[47] Garcia, Fernando, et al. "Data fusion for overtaking vehicle detection based on radar and optical flow." 2012 IEEE Intelligent Vehicles Symposium. IEEE, 2012.

[48] Garcia, Fernando, et al. "Sensor fusion methodology for vehicle detection." IEEE Intelligent Transportation Systems Magazine 9.1 (2017): 123-133. MLA

[49] Takizawa, Hiroomi, Kenichi Yamada, and Toshio Ito. "Vehicles detection using sensor fusion." IEEE Intelligent Vehicles Symposium, 2004. IEEE, 2004.

[50] Sifuentes, E., O. Casas, and R. Pallas-Areny. "Wireless magnetic sensor node for vehicle detection with optical wake-up." IEEE Sensors Journal 11.8 (2011): 1669-1676.

[51] Ma, Sai, et al. "Reliable Wireless Vehicle Detection using Magnetic Sensor and Distance Sensor." International Journal of Digital Content Technology and its Applications 8.1 (2014): 112.

[52] Treiber Martin, and Arne Kesting. "Trajectory and Floating-Car Data." Traffic Flow Dynamics. Springer, Berlin, Heidelberg, 2013. 7-12.

[53] Ke, Ruimin, et al. "A cost-effective framework for automated vehicle-pedestrian near-miss detection through onboard monocular vision." Proceedings of the IEEE Conference on Computer Vision and Pattern Recognition Workshops. 2017.

[54] Ke, Ruimin, et al. "Real-time bidirectional traffic flow parameter estimation from aerial videos." IEEE Transactions on Intelligent Transportation Systems 18.4 (2017): 890-901.

[55] Maerivoet, Sven, and Steven Logghe. "Validation of travel times based on cellular floating vehicle data." Proceedings of the 6th European Congress and Exhibition on Intelligent Transport Systems and Services, Aalborg, Denmark. 2007.

[56] Kerner, B. S., et al. "Traffic state detection with floating car data in road networks." Proceedings. 2005 IEEE Intelligent Transportation Systems, 2005. IEEE, 2005.

[57] Brockfeld Elmar, et al. "Benefits and limits of recent floating car data technology–an evaluation study." Proceedings of the 11th World Conference Transportation Research, Berkeley, CA. 2007.

[58] Rahmani, Mahmood, and Haris N. Koutsopoulos. "Path inference from sparse floating car data for urban networks." Transportation Research Part C: Emerging Technologies 30 (2013): 41-54.

[59] Bramberger, Michael, et al. "Real-time video analysis on an embedded smart camera for traffic surveillance." Proceedings. RTAS 2004. 10th IEEE Real-Time and Embedded Technology and Applications Symposium, 2004. IEEE, 2004.

[60] Duan, Bobo, et al. "Real-time on-road vehicle and motorcycle detection using a single camera." 2009 IEEE International Conference on Industrial Technology. IEEE, 2009.

[61] Alessandrelli, Daniele, et al. "ScanTraffic: smart camera network for traffic information collection." European Conference on Wireless Sensor Networks. Springer, Berlin, Heidelberg, 2012.

[62] Arnoul, P., et al. "Traffic signs localisation for highways inventory from a video camera on board a moving collection van." Proceedings of Conference on Intelligent Vehicles. IEEE, 1996.

[63] Ruta, Andrzej, et al. "In-vehicle camera traffic sign detection and recognition." Machine Vision and Applications 22.2 (2011): 359-375.

[64] Gavrila, Dariu M. "Traffic sign recognition revisited." Mustererkennung 1999. Springer, Berlin, Heidelberg, 1999. 86-93.

[65] Puri, Anuj. "A survey of unmanned aerial vehicles (UAV) for traffic surveillance." Department of computer science and engineering, University of South Florida (2005): 1-29.

[66] Gaszczak, Anna, Toby P. Breckon, and Jiwan Han. "Real-time people and vehicle detection from UAV imagery." Intelligent Robots and Computer Vision XXVIII: Algorithms and Techniques. Vol. 7878. International Society for Optics and Photonics, 2011.

[67] Kanistras, Konstantinos, et al. "Survey of unmanned aerial vehicles (UAVs) for traffic monitoring." Handbook of unmanned aerial vehicles (2015): 2643-2666.

[68] Wang, Liang, Fangliang Chen, and Huiming Yin. "Detecting and tracking vehicles in traffic by unmanned aerial vehicles." Automation in construction 72 (2016): 294-308.

[69] Ke, Ruimin, et al. "Real-Time Traffic Flow Parameter Estimation from UAV Video Based on Ensemble Classifier and Optical Flow." IEEE Transactions on Intelligent Transportation Systems (2018).

[70] Abad, F., et al. "Parking space detection." Proc. 14th World Congr. Intell. Transp. Syst (2007): 1-8.

[71] Mathur, Suhas, et al. "ParkNet: a mobile sensor network for harvesting real time vehicular parking information." Proceedings of the 2009 MobiHoc S 3 workshop on MobiHoc S 3. ACM, 2009.

[72] Kanaki, Shota, et al. "Cooperative moving-object tracking with multiple mobile sensor nodes—Size and posture estimation of moving objects using in-vehicle multilayer laser scanner." 2016 IEEE International Conference on Industrial Technology (ICIT). IEEE, 2016.

[73] Zhang, Boyu, et al. "Influence of heavy metal materials on magnetic properties of Pt/Co/heavy metal tri-layered structures." Applied Physics Letters 110.1 (2017): 012405.

[74] Finlay, Christopher Charles, et al. "International geomagnetic reference field: the eleventh generation." Geophysical Journal International 183.3 (2010): 1216-1230.

[75] Bokareva, Tatiana, et al. "Wireless sensor networks for battlefield surveillance." Proceedings of the land warfare conference. 2006.

[76] J.B. Calvert, “Electronics 30 – Phototubes” 2002

[77] Saghaei, Jaber, Ali Fallahzadeh, and Tayebeh Saghaei. "Vapor treatment as a new method for photocurrent enhancement of UV photodetectors based on ZnO nanorods." Sensors and Actuators A: Physical 247 (2016): 150-155.

[78] Schlyter, Paul. "Radiometry and photometry in astronomy." Online at http://stjarnhimlen. se/comp/radfaq. html 10 (2017).

[79] Gao, Lijun, Shengyi Liu, and Roger A. Dougal. "Dynamic lithium-ion battery model for system simulation." IEEE transactions on components and packaging technologies 25.3 (2002): 495-505.

[80] Hald, Jørgen, and Frank Jensen. Spherical near-field antenna measurements. Vol. 26. Iet, 1988.

[81] Sparkfun RFM69HCW Hookup Guide (https://learn.sparkfun.com/tutorials/rfm69hcw-hookup-guide/the-antenna)

[82] Padhi, Trilochan. "Theory of coil antennas." Journal of Research of the National Bureau of Standards (1965): 997-1001.